EUROPEAN ORGANIZATION FOR NUCLEAR RESEARCH

ADDENDUM–10 to PROPOSAL CERN/SPSC/P264

Progress Report and Beam Request for 2002

The NA49 Collaboration

Abstract

This document discusses the status of the analysis and physics results obtained by the NA49 experiment. For 2002 the collaboration maintains the request for 4 weeks of running with proton beams. Furthermore the collaboration requests 10 days of Pb beam at 20 and 30 A·GeV and the full period of Pb-beam at 158 A·GeV energy. Most of the Pb-beam period at full energy will be used for data taking with fragmentation deuterons.

S.V. Afanasiev[9], T. Anticic[19], D. Barna[5], J. Bartke[7], R.A. Barton[3], L. Betev[10],
H. Białkowska[17], A. Billmeier[10], C. Blume[8], C.O. Blyth[3], B. Boimska[17], M. Botje[1],
J. Bracinik[4], R. Bramm[10], R. Brun[11], P. Bunčić[10,11], V. Cerny[4], O. Chvala[15], J.G. Cramer[16],
P. Csató[5], P. Dinkelaker[10], V. Eckardt[14], P. Filip[14], H.G. Fischer[11], Z. Fodor[5], P. Foka[8],
P. Freund[14], V. Friese[13], J. Gál[5], M. Gaździcki[10], G. Georgopoulos[2], E. Gładysz[7], S. Hegyi[5],
C. Höhne[13], P.G. Jones[3], K. Kadija[11,19], A. Karev[14], V.I. Kolesnikov[9], T. Kollegger[10],
M. Kowalski[7], I. Kraus[8], M. Kreps[4], M. van Leeuwen[1], P. Lévai[5], A.I. Malakhov[9],
C. Markert[8], B.W. Mayes[12], G.L. Melkumov[9], A. Mischke[8], J. Molnár[5], J.M. Nelson[3],
G. Pálla[5], A.D. Panagiotou[2], K. Perl[18], A. Petridis[2], M. Pikna[4], L. Pinsky[12], F. Pühlhofer[13],
J.G. Reid[16], R. Renfordt[10], W. Retyk[18], C. Roland[6], G. Roland[6], A. Rybicki[7], A. Sandoval[8],
H. Sann[8], N. Schmitz[14], P. Seyboth[14], F. Siklér[5], B. Sitar[4], E. Skrzypczak[18], G.T.A. Squier[3],
R. Stock[10], H. Ströbele[10], T. Susa[19], I. Szentpétery[5], J. Sziklai[5], T.A. Trainor[16], D. Varga[5],
M. Vassiliou[2], G.I. Veres[5], G. Vesztergombi[5], D. Vranić[8], S. Wenig[11], A. Wetzler[10],
I.K. Yoo[13], J. Zaranek[10], J. Zimányi[5]

[1]NIKHEF, Amsterdam, Netherlands.
[2]Department of Physics, University of Athens, Athens, Greece.
[3]Birmingham University, Birmingham, England.
[4]Comenius University, Bratislava, Slovakia.
[5]KFKI Research Institute for Particle and Nuclear Physics, Budapest, Hungary.
[6]MIT, Cambridge, USA.
[7]Institute of Nuclear Physics, Cracow, Poland.
[8]Gesellschaft für Schwerionenforschung (GSI), Darmstadt, Germany.
[9]Joint Institute for Nuclear Research, Dubna, Russia.
[10]Fachbereich Physik der Universität, Frankfurt, Germany.
[11]CERN, Geneva, Switzerland.
[12]University of Houston, Houston, TX, USA.
[13]Fachbereich Physik der Universität, Marburg, Germany.
[14]Max-Planck-Institut für Physik, Munich, Germany.
[15]Institute of Particle and Nuclear Physics, Charles University, Prague, Czech Republic.
[16]Nuclear Physics Laboratory, University of Washington, Seattle, WA, USA.
[17]Institute for Nuclear Studies, Warsaw, Poland.
[18]Institute for Experimental Physics, University of Warsaw, Warsaw, Poland.
[19]Rudjer Boskovic Institute, Zagreb, Croatia.

1 Introduction

This report provides a summary of the status and future programme of the NA49 experiment at the CERN SPS. The history of the experiment is documented in a series of previous reports to the SPS Committee [1, 2, 3, 4, 5].

The primary purpose of the heavy ion programme at the CERN SPS is the search for evidence of a transient deconfined state of strongly interacting matter during the early stage of nucleus–nucleus collisions. The NA49 experiment [6] was designed for the investigation of hadron production in the most violent Pb+Pb interactions at the Cern SPS. With its large acceptance tracking and particle identification it is in addition an excellent detector for the study of nucleon–nucleus collisions of controlled centrality and of nucleon–nucleon reactions.

Data have been recorded on Pb+Pb collisions at 158, 80, and 40 A·GeV beam energy as well as smaller runs of C+C and Si+Si at 158 and 40 A·GeV. Moreover, extensive data sets were taken for hadron–nucleon (p+p, d+p, π+p) and hadron–nucleus (p+Pb, π+Pb) reactions. All raw data have been processed to the data summary tape status and are now in the process of physics analysis.

The status of physics analysis concerning elementary hadronic interactions is discussed in Section 2 with special emphasis on isospin effects and their consequences on the interpretation of heavy ion data. This concerns in particular the production of strange mesons as well as baryons and anti-baryons up to strangeness ± 3.

The NA49 programme concerning nucleus–nucleus collisions recently focused on the study of energy dependence of hadron production in central Pb+Pb collisions. The aim of this investigation is the search for anomalies in the energy dependence of experimental observables which may indicate the onset of deconfinement at low SPS energies. This status report presents selected results from the Pb runs at 40, 80 and 158 A·GeV in Section 3.1. These underline the importance of the completion of the energy scan programme this year with the approved low energy runs at 20 and 30 A·GeV.

High statistics data on central Pb+Pb collisions taken in 2000 are being analysed in a search for rare signals: open charm production, ϕ decay in the di-electron channel, Ω and anti-deuteron production. First preliminary results on these rare signals are presented in Section 3.2.

2 Results of Analysis of Hadron–Proton and Hadron–Nucleus Interactions

In the absence of a quantitative theory of soft hadronic interactions the interpretation of experimental results obtained in nucleus-nucleus collisions has to rely on a comparison with elementary hadron-hadron and hadron-nucleus reactions. As the heavy nuclei used in these studies have 60% neutron content, this comparison necessitates knowledge of hadronisation processes involving neutrons.

The behaviour of particle yields with respect to a rotation of the projectile isospin has not been studied experimentally in any quantitative detail. This behaviour will - in addition to the general concept of isospin symmetry - finally be governed by the hadronic production mechanisms involved. As will be shown below, the study of hadronic interactions with different projectile isospin will therefore offer more direct insight into the hadronization mechanism. The NA49 experiment has obtained in the years 1999/2000 pilot data with deuteron beam in order to provide data with neutron interactions. The inverse-kinematics deuteron+p configuration allows - by means of proton spectator tagging - the isolation of clean n+p collisions. We present here first results concerning final state pions, kaons, protons and anti-protons which allow scrutiny of the effects of projectile isospin rotation on particle yields, baryon and anti-baryon production and enhancement effects in kaon and cascade baryon production.

2.1 Experimental Procedure

The incoming Pb beam is fragmented into secondary nuclei in a 10 mm carbon target. Z/A=1/2 nuclei are selected by appropriate setting of the beam line. Out of a mass spectrum which is rapidly falling with A, deuterons are selected by pulse height window cuts on the analog signals from beam scintillation and proportional counters. The deuterons impinging on a liquid H2 target produce n+p (proton spectator), p+p (neutron spectator) and about 17% (n+p)+p interactions (no spectator). The n+p collisions can be cleanly isolated by selecting spectator protons imposing tight cuts on their transverse and longitudinal momenta. A selection of 120 k n+p events has thus been obtained. This event number is about a factor of 20 below the statistics available in p+p interactions.

2.2 Results on Charged Pions

Projectiles		n		p	
Produced particles	π^-		π^0		π^+
Isospin	-1		0		+1

The expected ("trivial") isospin symmetry in pion production i.e. the complete flip between π^+ and π^- yields when changing from proton to neutron projectile has not been measured to any precision in the SPS energy range. Results as a function of transverse momentum at fixed x_F are presented in Fig. 1 which shows that indeed charge reflection symmetry is achieved within statistical errors of a few percent over a wide range of p_T. This is extended to a wider x_F interval in Fig. 2 which shows p_T-integrated π^+/π^- resp. π^-/π^+ ratios as a function of x_F. Here two regions are of interest:

a) At low x_F π^-/π^+ should approach 1 in n+p interactions if charge reflection holds. This is borne out by the measurements shown in Fig. 2. The extent of the transition region in x_F offers a first determination of pion feed-over from target to projectile hemisphere. It is

2

visible that the feed-over is small already at $x_F = 0.05$ and vanishes at about $x_F = 0.1$. This result is important for some of the conclusions drawn below.

b) At large x_F the pionic charge ratios become large and therefore allow a more sensitive test of charge reflection symmetry which is not a priori implied by isospin invariance. The present data (see Fig. 2) cannot exclude such effects and it would be desirable to obtain similar statistical errors in n+p and p+p reactions.

2.3 Results on Charged Kaons

Due to strangeness conservation the situation is more complex for strange meson production. In fact kaons may be produced

a) in conjunction with hyperons ("associate production") and

b) in pairs.

Mechanism (a) can be described by the following isospin quadruplet:

			Strangeness
Projectiles	n	p	
Produced particles	K^0	K^+	1
	K^-	$\overline{K}^0$	-1
Isospin	-1/2	+1/2	

As in this process the s-quark is fixed in the hyperon, the K^+ yield ($\overline{s}$-quark) will not commute with the K^- yield (s-quark). K^- can only be produced here in the decay of Y^* (Σ^*) resonances which also yield $\overline{K}^0$. Consequently, in the "associate" hyperon-kaon channel, by exchanging p with n projectile, instead of $K^+ \leftrightarrow K^-$ the commutation $K^0 \leftrightarrow K^+$ and $\overline{K}^0 \leftrightarrow K^-$ should be dominant. This argument also raises questions about the isospin dependence of K^0_s production which "bridges" the multiplet by having both K^0 and $\overline{K}^0$ content.

The kaon pair production mechanism (b) corresponds to the following isospin triplet:

						Strangeness
Projectiles		n		p		
Produced particles	K^-K^0		K^+K^-		$K^+\overline{K}^0$	0
			$K^0\overline{K}^0$			
Isospin	-1				1	

In this case – and in analogy with the pion triplet discussed in the preceding section – one has to expect a definite dependence of charged kaon production on projectile charge: K^+ production should be reduced, K^- production enhanced when switching from p to n projectile. The relative weight of mechanisms (a) and (b) in charged kaon production is not predicted from soft QCD. It can be expected, though, that process (a) should dominate in the threshold region at low cms energy, whereas process (b) should become more and more important as energy increases.

NA49 has obtained the first comparative measurement of charged kaons with both p and n beams. Fig. 3 shows kaon yields as a function of p_T at two values of x_F in the projectile region. It is apparent that compared to the charged pions the charged kaons **do not** commute with projectile isospin. Within statistical errors on the contrary, both K^+ and K^- yield are invariant against projectile charge. This observation carries strong consequences for K/π ratios as shown

in Fig. 4 for K^+/π^+ and K^-/π^- from protons and neutrons as a function of x_F. Interpretation of K/π ratios from nuclei and their comparison to p+p interactions has therefore to take account of the proper isospin mixture in these nuclei. The necessary correction factors for Pb+Pb collisions are shown in Fig. 5: they reach (at 158 AGeV) values of up to 30%, depending on x_F. This is exemplified in Fig. 6 where K^+/π^+ and K^-/π^- ratios from Pb+Pb collisions as measured by NA49 are presented both uncorrected and corrected for isospin effects.

NA49 has also obtained K/π ratios from p+Pb interactions with controlled centrality. Here the comparison to the elementary p+p collisions is straight-forward in the p projectile hemisphere, but suffers from isospin effects in the backward (Pb) hemisphere. In the transition region around $x_F = 0$, in addition target-pile-up in this multiple collision process has to be taken into account. The measured K/π ratios are shown in Fig. 7 as a function of x_F. Target feedover effects are expected to reach out to about $x_F = 0.05$ (see above) and can be corrected for by using the approximate linearity of target yields with the number of collisions (see arguments discussed below in Chapter 7.2 with respect to proton and cascade yields).

The thus corrected K/π ratios are compared to Pb+Pb interactions in Fig. 8. Apparently, both for K^+ and K^- ratios there is - within statistical erors - **no difference** visible between both types of reactions, and this over the complete x_F range accessible to NA49. This constitues an important result for the interpretation of A+A collisions.

It would be of obvious interest to further reduce the statistical and systematic errors related to these particle ratios. NA49 has already doubled the event numbers in p+Pb interactions in 2001. Further running with n+p and p+p collisions is now mandatory.

2.4 Results on Protons and Anti-protons

In baryon production a clear distinction between "net" protons and neutrons which contribute to the overall baryon number balance and "pair produced" baryons has to be made. The latter should always be treated together with their partners as baryon number free systems.

2.4.1 Net Protons and Neutrons

Net baryons can be arranged in the following isospin doublets:

Projectiles	n	p
Produced particles	n	p
Isospin	-1/2	+1/2

Although an isospin-symmetric behaviour of neutrons and protons with respect to projectile charge seems obvious, the distribution of their cross sections over phase space is non-calculable and has therefore to be measured. In this respect the absence of reliable data on neutron production in p+p and proton and neutron production in n+p interactions is absolutely flagrant: hence a large uncertainty in properly predicting isospin-corrected baryon distributions for comparison with A+A data.

NA49 has performed a measurement of neutron production in p+p collisions and has obtained for the first time proton and anti-proton yields from n+p interactions. The results are given in Fig. 9. Discussing first the baryon cross sections it is seen (Fig. 9a) that indeed, as expected, the neutron yields from proton projectiles are equal to the proton yields from neutron projectiles. It should be stressed however that the shape of the measured x_F distributions is non-trivial and directly connected to production mechanisms. The fact that proton yields at $x_F = 0$

are closely similar in n+p and p+p collisions has to do with the mechanism of baryon number transfer (stopping) which carries direct relevance also for p+Pb and Pb+Pb reactions.

2.4.2 Pair Produced Baryons

The first ever measurement of anti-proton production in n+p interactions presented in Fig. 9b shows a sizeable increase of anti-proton yield from n projectiles. When taking account of the fact that in n+p events there is at $x_F \simeq 0$ a superposition from target protons and projectile neutrons (see arguments on π^+/π^- ratios above) the increase amounts to about 50%. This measurement has therefore immediate and rather profound consequences for the understanding of baryon pair production. Would pairs only be produced in the symmetric configurations $p\overline{p}$ and $n\overline{n}$ (isospin of the effective pair equal zero) this would mean a strong dependence of I=0 amplitudes on projectile isospin: there is no basis for this assumption. If however one allows for the presence of asymmetric pair configurations of the type $p\overline{n}$ or $n\overline{p}$ then $b\overline{b}$ pairs can be arranged in the following multiplet which resembles the isospin 1 triplet of pions:

Projectiles		n		p	
Produced particles	$\overline{p}n$		$p\overline{p}$ $n\overline{n}$		$p\overline{n}$
Isospin	-1		0		+1

Under this assumption and taking into account the observed charge reflection symmetry for pions the measured effect is easily understood as flip from the $p\overline{n}$ configuration into the $\overline{p}n$ configuration when interchanging p and n projectile. There is however a pecularity in the above multiplet: unlike π^+ and π^- protons and anti-protons turn also up in the I=0 symmetric configuration: the effect of any isospin reflection is therefore damped by this symmetric term. In this aspect the 50% excess of $\overline{p}$ in n+p corresponds to a very strong isospin correlation especially if compared to the 20% effect observed for π^+/π^- at $x_F = 0$. This and the fact that the effective mass of the baryon pairs is above 2 GeV indicates that the study of pair produced baryons gives access to more primordial phases of hadronization processes. Supporting evidence for this picture comes from Lear experiments which were able to isolate in the inverse process $p\overline{p}$ $\rightarrow$ mesons final state high mass/high spin mesonic resonances.

NA49 would definitely benefit from enhanced statistics in both p+p and especially n+p interactions in pursuing this cycle of studies.

2.4.3 Baryon Pair Production with Pion Beams

The above results have been augmented by measurements of baryon and anti-baryon production with pion beams:

Projectiles	π^-		π^+
Produced particles	$\overline{p}n$	$p\overline{p}$ $n\overline{n}$	$p\overline{n}$
Isospin	-1	0	+1

In experiments with pion beams one may use the fact that there should be no "net" baryon number produced in the hadronization of the projectile in order to isolate the contributions from

the target proton. This is done by defining an "average pion" projectile $0.5 \cdot (\pi^+$ beam $+ \pi^-$ beam). By subtracting the thus averaged baryon yields from the pion beam results the p target contribution is eliminated and one is left with baryon pair production from the pion projectile. In addition by using the difference p–$\overline{\text{p}}$ one may eliminate the I=0 symmetric pair component. The result presented in Fig. 10 shows again several important features of baryon pair production:

a) There is a strong component of asymmetric p$\overline{\text{n}}$ and n$\overline{\text{p}}$ configurations.

b) This component commutates with projectile isospin.

c) The production mechanism of p$\overline{\text{p}}$ pairs becomes directly visible: the baryon/anti-baryon yields are not peaked at $x_F = 0$ but show a broad structure centered at $x_F \simeq 0.2$ for pion beams, indicating a non-central production of the corresponding heavy mesonic parent states reaching out to high x_F values.

2.5 Results Expected for Strange/Antistrange Baryon Production

In the following argumentation the above findings will be extended to the expected isospin dependence of strange and multistrange baryons. This should become experimentally accessible with better event statistics from n+p and p+p interactions.

Starting with the isospin multiplet structure for hyperon pair states (making no difference in notation between Λ^0 and Σ^0 which are anyway indistinguishable in most experiments)

		n		p		Strangeness
Projectiles		n		p		
Produced particles	$\Lambda\overline{\Sigma}^-$ $\Sigma^-\overline{\Lambda}$		$\Lambda\overline{\Lambda}$		$\Lambda\overline{\Sigma}^+$ $\Sigma^+\overline{\Lambda}$	-1+1
Isospin	-1		0		+1	

it becomes apparent that - due to the possible combination of isospin singlet states ($\Lambda, \overline{\Lambda}$) with the isospin triplet of Σ states the isospin rotation of n and p projectiles should always yield the same number of pair produced neutral hyperons. Therefore, unlike in the case of anti-protons, anti-lambdas measure the complete yield of pair produced hyperons and, as a consequence, the difference $\Lambda - \overline{\Lambda}$ gives the correct number of "net" hyperons independent of projectile type, again in sharp contrast to the difference p–$\overline{\text{p}}$.

Verification of this prediction needs more n+p events.

Proceeding now to cascade hyperons, the following table applies:

		n		p		Strangeness
Projectiles		n		p		
Produced particles	$\overline{\Xi}^0\Xi^-$		$\Xi^0\overline{\Xi}^0$ $\Xi^-\overline{\Xi}^+$		$\Xi^0\overline{\Xi}^+$	-2+2
Isospin	-1		0		+1	

This shows complete charge-antisymmetry with respect to the iso-doublet formed by proton/anti-proton. Therefore, comparing e.g. Pb+Pb to p+p collisions, $\overline{\Xi}^+$ should be suppressed, Ξ^- enhanced by simple isospin composition. This will be quantified in the following chapter.

						Strangeness
Projectiles		n		p		
Produced particles			$\Omega^-\overline{\Omega}^+$			-3+3
Isospin	-1		0		+1	

Ω^- and $\overline{\Omega}^+$ form finally isospin singlets (see table on top) and should therefore, like $\Lambda/\overline{\Lambda}$, not be affected by projectile isospin.

The possibility of strangeness-asymmetric pair combinations can however not be excluded here. As the yield ratios between $p/\Lambda/\Xi/\Omega$ production are about $1/10^{-1}/2\cdot 10^{-3}/10^{-4}$ such terms should in fact become more and more probable with decreasing cross section. Combinations like e.g. $\Omega^-/\overline{\Xi}^+$ or $\Xi^-/\overline{\Sigma}^+$ (plus evidently additional kaons) have to be taken into account.

The measurement of baryon production up to strangeness ± 3 in elementary production is therefore a pre-requisite for the interpretation of nuclear baryonic data. The NA49 experiment has produced, in addition to data on p,$\overline{p}$ and Λ,$\overline{\Lambda}$ a first ever measurement of Ξ^- and $\overline{\Xi}^+$ yields in p+p interactions at 158 GeV/c.

Ω^- production just becomes accessible with the available number of events. From the current statistics approximately 45 Ω^- may be extracted as shown in Fig. 11. This represents a 3.5 σ significant signal over background measurement. Doubling the events statistics will allow to improve the measurement to 5 σ and to extract a reliable Ω^- cross-section.

Currently there is no signal visible for the $\overline{\Omega}^+$. However, with the presently measured Ω^- signal, we can test the level of exclusion of the $\overline{\Omega}^+/\Omega^-$ ratio. With a 95% confidence level, this ratio is below 0.5. With two times higher statistics and assuming no $\overline{\Omega}^+$ signal, we will be able to exclude at the same confidence level a ratio above 0.35.

The situation may be summarized in Fig. 12 where anti-baryon/baryon ratios are shown up to strangeness ± 3 for p+p collisions. There seems to be an almost linear increase of the $\overline{b}/b$ ratios with strangeness content, leaving the possibility - by extrapolation to $\overline{\Omega}/\Omega$ - of a ratio of order 1 at S=± 3. The upper limit obtained for $\overline{\Omega}^+$ production excludes already such an extrapolation. The complex situation is further highlighted by the fact that practically all available microscopic production models predict very large $\overline{\Omega}^+/\Omega^-$ ratios in p+p collisions ranging up to factors of 2 and more [7].

2.6 Comparison of Cascade Baryon Production in p+p, p+Pb and Pb+Pb collisions

In the following the problems of comparison between different hadronic processes, of isospin effects and of the interpretation of "enhancement" effects will be exemplified for the case of cascade baryon production.

Measurements of cascade baryon cross sections are available from the WA97 [8] and NA49 [9] experiments at the SPS and are given in Table 1. These measurements fortunately enough cover a wide range of hadronic interactions with a welcome overlap which allows control of consistency. The table also contains two very important normalisation and reference numbers: the number of "wounded nucleons" NW and the number of collisions ν per projectile nucleon characterizing each reaction.

	pp	pBe	pPb	pPb	pPb	PbPb	PbPb
	NA49	WA97	WA97	NA49	NA49	WA97	NA49
NW	2	2.5	4.7	4.7	6.7	350	362
ν	1	1.5	3.7	3.7	5.7	4.5	4.5
Ξ^-	0.00074	0.0015	0.003	0.004	0.0058	1.5	1.49
$\overline{\Xi}^+$	0.00036	0.00068	0.0012	0.0014	0.0018	0.37	0.33

Table 1:

2.6.1 Comparison of Pb+Pb and p+p Interactions

Dividing the cascade yields in Pb+Pb collisions by the number of participant pairs (equal NW/2) one obtains, now seen per participant pair collision, and averaging over the NA49 and WA97 results (which agree within their 15% error limits) the following central rapidity densities:

			isospin corrected	
	Ξ	$\overline{\Xi}$	Ξ	$\overline{\Xi}$
p+p	0.00074	0.00036	0.00096	0.00028
Pb+Pb	0.0082	0.0019		
PbPb/pp	11.0	5.3	8.54	6.8

The above ratios constitute (a) a very sizeable cascade baryon enhancement and (b) a difference of a factor of two in enhancement between baryon and anti-baryon. The difference in isospin composition between p+p and Pb+Pb collisions should however, as discussed in chapter 6 above, be taken into account. It has been shown that one has - at least for Ξ pair production, to expect a decrease in $\overline{\Xi}$ and an increase in Ξ yield when switching from p to n projectile. Assuming this isospin effect to be of the same order as the one for protons/anti-protons quantified in Chapter 5 as about 1.5, the resulting net correction factor for the elementary nucleon+ nucleon collision would be $(0.6 \cdot 1.5 + 0.4 \cdot 1.0) = 1.3$. The application of this correction changes the enhancement of Ξ^- and $\overline{\Xi}^+$ to 8.5 and 6.8 respectively. As a consequence, the difference in baryon and anti-baryon enhancements is drastically reduced.

It should be clear from this example that the measurement of Ξ and $\overline{\Xi}$ cross sections in both p+p and n+p collisions is absolutely necessary for argumentations about the excess of cascade production in A+A reactions.

2.6.2 Comparison of p+A and p+p Interactions

Contrary to the symmetric nucleon+nucleon and nucleus+nucleus interactions discussed above, the hadron+nucleus collisions are by construction asymmetric. At a given impact parameter the projectile hadron will hit ν target nucleons (see table 1 above). The projectile fragmentation will thus be characterized by hadronization after multiple collisions, as is the case for *all* participating nucleons in a nucleus+nucleus interaction. The "wounded" target nucleons in a p+A reaction on the contrary are only hit once and are therefore - in their fragmentation - characterized by single collision physics i.e. close to the elementary nucleon+nucleon interaction. The final state hadron density will therefore have two components: a target component

which is the approximate sum of ν elementary hadronisation processes and a projectile component which carries the imprint of multiple (ν) collisions. Only the latter component should be comparable to nucleus+nucleus interactions.

The NA49 experiment has been able to check the superposition argument evoked above for the target component in the specific case of net baryon production in p+Pb collisions. Using data from both π^++Pb and π^-+Pb interactions which have no "net" baryon content on the projectile level (see also argumentation concerning π^++p and π^-+p in chapter 5 above) one can use the quantity p–$\overline{\text{p}}$ in order to measure directly the evolution of target baryon density with the number nu of collisions. The result of this measurement is given in Fig. 13. Here the net proton density is plotted as a function of x_F for p+p collisions and average π+Pb collisions at two different impact parameters corresponding to 2.2 and 4.7 projectile collisions. The approximate linearity of yield against ν at $x_F = 0$ is evident.

This observation allows to set up a simple superposition formula for particle yields at xF=0 in p+A collisions:

$$(dn/dx)^{p+A}_{x_F=0} = (dn/dx)^{p+p}_{x_F=0} \cdot (0.5 \cdot (\nu \cdot \alpha) + 0.5 \cdot E),$$

where the "enhancement factor" E describes the deviation of the projectile component (multiple collisions) from the simple p+p behaviour (single collision) and the parameter α the influence of isospin effects on particle yield due to the composition of A from by protons and neutrons.

This formula demonstrates clearly that with increasing number of collisions the relative weight between target "pile-up" and projectile fragmentation becomes bigger and bigger contrary to A+A collisions where this formula should read:

$$(dn/dx)^{A+A}_{x_F=0} = (dn/dx)^{N+N}_{x_F=0} \cdot (0.5 \cdot E + 0.5 \cdot E) \cdot NW/2.$$

The visibility of any enhancement effect due to multiple collisions is therefore strongly suppressed in p+A in comparison to A+A collisions for central x_F (see argumentation of Chapter 4 for kaon production).

By applying the above formalism the cascade baryon measurements of table 1 in p+A interactions can now be confronted with both the elementary p+p and the multi-collision Pb+Pb results and the enhancement factors E extracted from the data, see Fig. 14. From this figure two conclusions may be drawn:

a) With or without taking into account isospin effects the cascade yields measured in Pb+Pb collisions comply within experimental errors with the ν-dependence extrated from p+p and p+Pb interactions.

b) The application of isospin effects of the expected order of magnitude reduces the difference between $\overline{\Xi}^+$ and Ξ^- enhancements both in p+Pb and Pb+Pb reactions.

Both findings agree with what has been concluded in Chapter 4 for K meson production.

It is clear that - in order to replace conjecture by reality as far as isospin effects are concerned - the measurement of $\overline{\Xi}^+$ and Ξ^- with neutron beam is a necessity. This is what NA49 proposes to do in 2002.

2.7 Improvement of Data Taking Efficiency by Triggering on Proton Spectators

The pilot run with deuteron beam in 1999 used the standard NA49 triggering scheme with the addition of a pulse height cut as described above. Spectator selection was done off line once the complete data sample was processed.

For future deuteron beam running the data taking efficiency may be improved by a factor of about 4 by introducing an on-line trigger on spectator protons. Due to their small p_T values (≤ 100 MeV/c) and their small spread in longitudinal momentum these are confined to a tiny area of only a few cm in diameter in the downstream part of the experiment. A scintillation counter of the required size (together with a newly constructed proportional chamber with 100 μm space resolution) will allow for fast triggering on proton spectators and a precision measurement of their momentum.

The expected number of events in the 23-day period of 160 AGeV Pb-beam foreseen in 2002 would thus allow to collect about 1.6 Mevents on DST. This event sample compares favourably with the 2.5 M events currently available from p+p interactions. It would contain more than 400 Ξ^- and more than 100 $\overline{\Xi}^+$ (already including the expected reduction of $\overline{\Xi}^+$ yield by isospin effects) which should allow a sensible determination of the baryon cross sections and of baryon/anti-baryon ratios up to cascades. In addition the arguments developed above concerning meson production could be quantified to a statistical accuracy comparable to p+p collisions.

2.8   Status of p+p and p+Pb Event Samples and Analysis

NA49 has proposed in October 2000 a programme of data taking with p+p and p+A interactions reaching over three years up to the end of 2003, requesting 4 weeks of proton beam per year. The SPSC has granted a period of 28 days in 2001. In preparation of this data taking the NA49 detector was upgraded by the construction of a new TPC which closes the acceptance hole at $x_F \geq 0.5$ imposed in the standard TPC setup by the presence of the Pb-beam in Pb+Pb running.

In accordance with the plans put forward, data taking was arranged as follows:

p+Pb at 160 GeV/c: 1 480 000 events $\rightarrow$ 1 000 000 events on DST
p+Pb at 100 GeV/c: 850 000 events $\rightarrow$ 590 000 events on DST

These two items fulfill the plans for doubling up the available event number in p+Pb at different centralities and of studying energy dependence. It is evident that these new data constitute a large amelioration for the analysis presented above. In addition, further data with pion beams have been obtained:

π^-+Pb at 160 GeV/c: 790 000 events $\rightarrow$ 550 000 events on DST
π^++Pb at 160 GeV/c: 420 000 events $\rightarrow$ 290 000 events on DST

Data processing of the π^-+Pb sample has already been performed and results have entered the physics results shown above.

In addition, NA49 was able to benefit of 13 days of p beam with the special LHC spill structure. These data have reduced duty cycle and are in principle not well adapted to detectors with long open time like the NA49 TPC system. Using the detailed beam timing information available in NA49 and special background rejection techniques it has been nevertheless possible to collect efficiently the following data:

p+p at 160 GeV/c: 1 100 000 events $\rightarrow$ 550 000 events on DST (special spill)

All these new data will be processed in the near future and will enter into the continuing data analysis which is being actively pursued. It should be evident from the above physics argumentation that a further sizeable increase in p+p statistics, as it has been requested in 2000, will be of great benefit for most of the physics subjects studied and is indeed our next priority. This should help to obtain measured cross sections also for Ω^- and $\overline{\Omega}^+$ to give only one example.

3 Selected Results from the Study of Nucleus–Nucleus Collisions

3.1 Energy Dependence

The results from the heavy-ion program at CERN indicated that deconfinement may set in within the SPS energy range [10],[11]. Within most model scenarios the data imply that the initial energy density exceeds the critical value. Originally proposed signatures [12] of the QGP were observed in Pb+Pb collisions at the top SPS energy, i.e. J/Ψ suppression, strangeness enhancement, and possibly thermal photons and dileptons. The significance of these signals as QGP signatures has come under renewed scrutiny. Moreover, there is no observational evidence for a sharp phase transition from QGP to hadrons such as phase coexistence [13], critical fluctuations [13, 14] or more speculative effects like DCC [15] or parity violation [16].

The NA49 experiment is performing an energy scan from 20–158 A·GeV in an effort to strengthen the evidence for the onset of deconfinement by searching for anomalies in the energy dependence of experimental observables. Data at 40, 80 and 158 A·GeV have so far been recorded and analysed and selected preliminary results are presented below.

3.1.1 Yields of π, K, Λ and $\bar{\Lambda}$

Raw K^+ and K^- yields were extracted from fits of the distributions of dE/dx and TOF (where available) in narrow bins of rapidity y and transverse momentum p_T. The resulting spectra were then corrected for geometrical acceptance, losses due to in–flight decays and reconstruction efficiency. The latter was determined from embedding simulated tracks into real events and amounted to $\approx 95\%$. Spectra of π^- mesons were derived from the acceptance corrected negatively charged particle yields in p_T and y (assuming the π mass) by subtracting the estimated contribution of K^-, $\bar{p}$ and the contamination from secondary hadron decays. The ratio π^+/π^- was determined in the region where both dE/dx and TOF are available (0.91, 0.94 and 0.97 at 40, 80 and 158 A·GeV) and was assumed to be y independent.

The resulting rapidity distributions of π^- are plotted in Fig. 15. The integrated yields are 312±15, 445±22 and 610±30 at 40, 80 and 158 A·GeV respectively. Pions are the dominant produced particle species and thus their number provides a measure of the entropy in a statistical model description of the reaction. The yield of pions (estimated here as $\langle \pi \rangle = 1.5 \cdot (\langle \pi^- \rangle + \langle \pi^+ \rangle)$) divided by the number of wounded nucleons (participants) N_W is shown versus the Fermi energy variable $F \equiv (\sqrt{s} - 2m_N)^{3/4}/\sqrt{s_{NN}}^{1/4} \approx s_{NN}^{1/4}$ in Fig. 16. While p+p data show a linear rise throughout there is a change for A+A collisions (illustrated more clearly in the inset) in the SPS energy range. Below one finds a regime of slight suppression, above a region of enhancement with a steeper linear rise than for p+p reactions. This steepening must be due to collective effects and may be interpreted as indicating the activation of a large number of partonic degrees of freedom at the onset of deconfinement [17].

Kaons contain about 75% of the $s, \bar{s}$ quarks in the produced hadrons at SPS energies and thus their number indicates the total strangeness content of the final state. The rapidity distributions are displayed in Fig. 17 and integrate with small extrapolation to total yields of 18±1,

11

29±2, 50±5 for K$^-$ and 56±3, 79±5, 95±9 for K$^+$ at 40, 80, 160 A·GeV respectively. Yields of most particles, of course, increase with energy. Changes in the composition of the produced system are better characterised by particle ratios. Measurements of K$^-$/π^- and K$^+$/π^+ at midrapidity from NA49 are plotted versus energy in Fig. 18 and compared to results at lower and higher energies. A continuous increase is seen for K$^-$/π^-. For K$^+$/π^+ one finds a steeper rise followed by a maximum at the lower end of the SPS energy region and a gradual decrease. Within a reaction scenario based on nucleon–nucleon collisions these features might be attributed to thresholds and the decrease of the baryon density with increasing energy. The ratio K$^-$/π^- exhibits the threshold of the K$\bar{\text{K}}$ production mechanism. The lower mass threshold of associate KY production leads to a steeper rise in K$^+$/π^+ and the rapidly falling baryon density may result in a compensation of the declining contribution from the KY by the growing contribution from the K$\bar{\text{K}}$ production mechanism. It will be interesting to see whether the excitation function of the K/π ratio in nucleon–nucleon collisions supports such an interpretation.

The most abundantly produced hyperons are Λ and $\bar{\Lambda}$ for which Fig. 19 shows the rapidity distributions. These show a broad shape for Λ reflecting the associate production mechanism and the partially stopped participant nucleon distribution. In contrast the distribution is of narrower Gaussian type for $\bar{\Lambda}$ which are most likely produced as members of hyperon–anti-hyperon (Y$\bar{\text{Y}}$) pairs. The ratios $\langle\Lambda\rangle/\langle\pi\rangle$ and $\langle\bar{\Lambda}\rangle/\langle\pi\rangle$ of 4π integrated yields are displayed as a function of energy in Fig. 20. One observes a steep threshold rise for the $\langle\Lambda\rangle/\langle\pi\rangle$ ratio followed by a decline which can be mainly attributed to the rapidly decreasing net baryon density. The ratio $\langle\bar{\Lambda}\rangle/\langle\pi\rangle$ exhibits a continuous rise due to the high mass Y$\bar{\text{Y}}$ threshold.

It is apparent from Fig. 19 that the hyperon rapidity coverage of NA49 which is complete at 40 A·GeV beam energy shrinks to about half the available phasespace for 158 A·GeV. In order to improve on this situation it is proposed to take data with a modified detector configuration during part of the 2002 full energy Pb-beam run. A reduction of the magnetic field combined with a target position closer to the first TPC will extend the coverage in the backward hemisphere close to target rapidity ($-2.2 \leq y_{cms} \leq -1.5$). This will allow a determination of the Λ multiplicity in full phase space with only small extrapolation and systematic uncertainty also at the top SPS energy.

Since anti-hyperon production rates are small and isospin symmetry approximately holds ($\langle\text{K}^+\rangle \approx \langle\text{K}^0\rangle$) nearly half of the $\bar{s}$ quarks in the produced hadrons are contained in K$^+$ mesons. Moreover, strangeness conservation requires $\langle s \rangle = \langle \bar{s} \rangle$. Thus $\langle\text{K}^+\rangle$ measures to a good approximation one quarter of all s and $\bar{s}$ quarks in the final state hadrons. The energy dependence of the $\langle\text{K}^+\rangle/\langle\pi^+\rangle$ ratio (see Fig. 21 left) therefore indicates a maximum in the fraction of strangeness carrying particles in the lower SPS energy range.

Microscopic dynamical and statistical models have been used extensively to describe particle yields in a wide variety of reactions. The first class is often based on string excitation, fusion and hadronization (e.g. HSD [18], RQMD [19], UrQMD [20]) followed by re-interactions of the formed hadrons (RQMD, UrQMD). As seen from Fig. 18 HSD does not reproduce the energy dependence of the midrapidity K$^+$/π^+ ratio. On the other hand, RQMD correctly predicts the trend, but somewhat over-predicts the ratio in the SPS energy range.

A comparison with the 4π ratio $\langle\text{K}^+\rangle/\langle\pi^+\rangle$ is presented in Fig. 21 left. Both UrQMD and RQMD get the steep threshold rise. UrQMD values are much too low in the plateau due to an over-prediction of pions. RQMD does not follow the drop in the SPS range which is indicated by the measurements.

The statistical hadron gas model as such makes no prediction concerning the energy dependence of particle production. However, it has recently been supplemented [21] by a parameterisation of the energy dependence of its two main parameters, baryo-chemical potential μ_B

and temperature T. Predictions are shown in Fig. 21 left for $\langle K^+\rangle/\langle\pi^+\rangle$ and Fig. 20 right for $\langle\Lambda\rangle/\langle\pi\rangle$. The trend of the data is well reproduced by this extended statistical hadron gas model calculation. In detail the decrease in the SPS energy range of both $\langle K^+\rangle/\langle\pi^+\rangle$ and $\langle\Lambda\rangle/\langle\pi\rangle$ and even more so of $\langle\Xi\rangle/\langle\pi\rangle$ (not shown) is not well described.

Predictions have also been published for a statistical model of the early stage which explicitly assumes formation of a transient deconfined phase above a certain threshold energy [17]. In this model the strangeness to entropy ratio is assumed to be established initially and to persist through the hadronization stage. A measure of this quantity is the ratio $E_s = (\langle\Lambda\rangle + \langle K + \bar{K}\rangle)/\langle\pi\rangle$ evaluated from the final hadron multiplicities which is plotted in Fig. 21 right. After a rise corresponding to the purely hadronic reaction in the model, one observes a saturation at the a level consistent with the strangeness to entropy ratio expected for an initially deconfined system.

3.1.2 $\pi\pi$ correlations

Correlations of pions with near equal momenta $\mathbf{p}_1$, $\mathbf{p}_2$ provide information on the size and internal dynamics of the fireball source at freeze–out [22]. The analysis was performed in the longitudinally comoving reference frame, decomposing the momentum difference $\mathbf{Q} = \mathbf{p}_1 - \mathbf{p}_2$ into long, side, out components. For $\pi^+\pi^-$ pairs the correlation peak at small Q is predominantly due to the Coulomb attraction and can be well reproduced by a Coulomb wave calculation [23] using the measured effective source size. Correlations of $\pi^-\pi^-$ are described by a product of parameterised Coulomb repulsion [23] and the quantum statistics enhancement, fitted with a Gaussian parameterisation. The resulting radius parameters R_{side}, R_{out}, R_{long} are plotted in Fig. 22 versus the average transverse momentum K_T of the pair. No striking energy dependence is observed. Within expanding source models the decrease with K_T is a manifestation of the strong longitudinal (R_{long}) and radial (R_{side}, R_{out}) collective flow at SPS energies. Moreover, there is little change in the lifetime $\tau_0 \approx R_{long}\sqrt{T/M_T}$ or the emission duration $\Delta\tau^2 \approx (R_{out}^2 - R_{side}^2)/\beta_T^2$ of the source. The small value of $\Delta\tau$ does not indicate a soft point of the matter equation of state of the kind discussed in ref. [13] near the onset of deconfinement.

3.1.3 Charge fluctuations

Recently it was proposed that event–by–event fluctuations of the charge ratio $R=N_+/N_-$ or the net charge $Q=N_+-N_-$ may be sensitive to deconfinement in the early stage of nucleus–nucleus collisions [24, 25]. The smaller charge quanta in a partonic phase are expected to result in a reduction of such fluctuations.

The fluctuations of the charge ratio were investigated via the measure $\tilde{D}$ [26] which is corrected for the residual net charge in the considered rapidity interval Δy as well as for global charge conservation. The preliminary NA49 results are shown in Fig. 23 left and are found to be close to the expectation for independent particle emission plus global charge conservation ($\tilde{D} \approx$ 4) and do not change significantly with energy. No evidence is seen for the reduction predicted for a resonance gas nor for the large decrease expected for a QGP phase. It is, of course, not clear whether reduced fluctuations in the QGP will persist through the hadronization, rescattering [27] and resonance decay [28] stages.

The quantity Φ_q was proposed in ref. [29] for studying fluctuations of the net charge. It is independent of the number of superimposed particle sources and event–by–event fluctuations of this number. It has value zero for independent particle emission and -1 for local charge conservation. Preliminary NA49 measurements are plotted in Fig. 23 right ver-

sus the ratio $\langle N_{ch} \rangle / \langle N_{ch} \rangle_{tot}$ of the multiplicity in the acceptance window and the total multiplicity in the events. Again no significant energy dependence is observed and the results are close to the prediction for independent particle emission plus global charge conservation $\Phi_q^{cc} = \sqrt{1 - \langle N_{ch} \rangle / \langle N_{ch} \rangle_{tot}} - 1$ (ref. [28], line in Fig. 23).

3.1.4 Anisotropic flow

Anisotropic flow in non-central collisions is sensitive to pressure in the early stage of the reaction, which can transform the initial space anisotropy of the reaction zone into an azimuthal anisotropy of the momentum distribution of the observed particles. The onset of deconfinement might result in a minimum of this effect [13]. Anisotropic flow is quantified by the Fourier coefficients v_n of the distribution of particle azimuthal angles Φ with respect to the reaction plane Ψ [30]:

$$v_n = \langle cos(n(\Phi_i - \Psi_n)) \rangle = \sqrt{2} \langle sin(n \cdot \Phi_i) \cdot sin(n \cdot \Psi_n) \rangle$$

Corrections for reaction plane resolution, nonuniform azimuthal acceptance and momentum conservation were applied. The results for v_1 (directed flow) and v_2 (elliptic flow) for pions are plotted versus rapidity in Fig. 24. The values for v_1 decrease from 40 (left) to 158 (right) A·GeV by a factor of 2, whereas v_2 shows a slight increase.

3.1.5 Summary

The study of central Pb+Pb collisions in NA49 at 40, 80 and 158 A·GeV led to the following conclusions:

- the produced number of pions per participant in Pb+Pb collisions changes from suppression with respect to p+p reactions to enhancement in the SPS energy range
- the fraction of produced particles containing s or $\bar{s}$ quarks passes through a maximum at low SPS energies
- strangeness production starts to be under-saturated with respect to statistical equilibrium at SPS energies at a level consistent with the deconfinement hypothesis
- no unusual features are found in the evolution of other characteristics of the produced hadron system

NA49 intends to close the data gap between existing measurements at the AGS and the SPS with the approved runs at 20 and 30 A·GeV in 2002.

3.2 Rare Signals

During the full energy Pb run in 2000, the NA49 experiment registered 3M central Pb+Pb collisions at 158 A·GeV. In order to increase the number of events per spill the running conditions and the DAQ system were optimised for this purpose. All registered events were reconstructed in summer 2001 after an additional calibration effort and the introduction of necessary reconstruction software modifications.

One goal of this study is to set an upper limit or observe a first positive signal of rare processes like production of open charm and vector mesons ϕ and possibly ω via the dielectron decay channel. Large event statistics are also required to study the production of Ω, light (anti)nuclei and resonances.

3.2.1 Open Charm

Open charm production in A+A collisions is an interesting and unexplored subject for experimental study. The measurement of the open charm yield provides a unique possibility to confront pQCD–based and statistical models of strong interactions [31].

The basic channels considered in the NA49 open charm search are:

$$D^0 \to \pi^+ + K^- \quad \text{and} \quad \bar{D}^0 \to \pi^- + K^+. \tag{1}$$

In the analysis the invariant mass is calculated for all combinations of a positively and a negatively charged track, assuming one to be a kaon and the other a pion. Given the large track multiplicity in each event (~ 1000 for a central event) the combinatorial background is clearly the main challenge in the analysis. This background is reduced by use of particle identification (dE/dx, TOF) and by applying appropriate cuts on single track and pair characteristics.

The resulting mass distribution after background subtraction is presented in Fig. 25 (left). The background was subtracted by fitting a (3rd order) polynomial to the region outside the D peak. Clearly, no D^0 signal has been detected. The total content of the four bins which contain the D^0 peak, is (0.20 ± 0.54) $D^0 + \bar{D}^0$ per event. This can be translated into an upper limit of 1.4 $D^0 + \bar{D}^0$ per event (95% CL).

In Fig. 25 (right) the upper limit for D^0 production as determined in the present analysis (square), is compared to various predictions of the D^0 yield. The two extreme models in the plot are charm production from an equilibrated QGP[31] (highest) and scaling of the yield measured in p–p by $A^{4/3}$, as predicted for a hard partonic process (lowest prediction). The other two models [32],[33] both use the measured J/ψ yields and different hadronization models to calculate the charm yield. The present result clearly excludes the equilibrated QGP [31] and the ALCOR hadronization model [33].

Also shown in the figure is the result without the use of the recent sample of 3M events (dot), demonstrating the increase in sensitivity obtained with the high statistics data.

3.2.2 ϕ production via the $\phi \to e^+ + e^-$ channel

After correction for the decay branching ratio there is a large difference (a factor of several) between the ϕ yields measured in central Pb+Pb collisions at 158 A·GeV via the $\phi \to K^+ + K^-$ [34] and $\phi \to \mu^+ + \mu^-$ [35] decay channels. In an attempt to understand the origin of this difference, NA49 started to study ϕ production in the dielectron channel, which is in principle accessible to the experiment.

Electrons and positrons are identified using dE/dx information and their invariant mass is calculated. In order to minimise the large combinatorial background, cuts on single track and pair properties are applied. The resulting invariant mass spectrum after background subtraction is presented in Fig. 26 (left). No ϕ signal is observed. The total content of the bins containing the ϕ peak is (4.8 ± 5.8) per event using the standard decay branching ratio. The estimated upper limit for the ϕ multiplicity obtained from the $\phi \to e^+ + e^-$ channel is shown in Fig. 26 (right) by the open (1996 data, 800K events) and full (2000 data, 2.4M events) squares. These preliminary upper limits are below the results from the $\phi \to \mu^+ + \mu^-$ channel [35], but consistent with the NA49 measurement [34] based on the $\phi \to K^+ + K^-$ channel.

3.2.3 Ω production

The Ω plays a prominent role for the understanding of heavy ion reactions. So far, only one measurement by the WA97 collaboration exists, which covers the acceptance region close to

mid-rapidity [36]. The large acceptance of the NA49 experiment together with the now available high statistics for central Pb+Pb events allow to determine the Ω and $\bar{\Omega}$ yield over a larger region of phasespace. Fig. 27 shows an example of the observed $\Omega + \bar{\Omega}$ signal, as obtained from a preliminary analysis of 500k events.

4   Beam Request for 2002

Based on the above progress report, on the status of data analysis, on the discussion of scientific priorities, and on the prospects for enhanced physics output, the NA49 collaboration proposes the following request for running in 2002:

4.1   Proton Beam at 158 GeV/c

In continuation of the programme presented in 2000 the collaboration maintains the request for 4 weeks of running with proton beam at 158 GeV/c to be used for doubling the event statistics of p+p interactions.

4.2   Completion of Energy Scan with 20 and 30 A·GeV

In the recent schedule of the SPS the number of days of low energy (20 and 30 A·GeV) Pb-beam time was reduced from originally 10 to 7 days. These changes, if confirmed, would have a serious impact on our physics programme. In a memorandum to the SPSC [37] we give the arguments which lead us to reiterate our request for a 10 day long low energy Pb running period.

4.3   Pb Beam at 158 A·GeV for the Study of Low Rapidity Λ-Hyperons

A few days of running with central Pb+Pb collisions using a reduced magnetic field and distance of the target to the first TPC in order to extend the acceptance coverage for Λ-Hyperons.

4.4   Deuteron Fragmentation Beam Derived from 158 A·GeV Pb-Projectiles

For most of the full energy Pb-beam period the collaboration proposes to take n+p data using a deuteron beam from fragmentation. By on-line triggering on the spectator protons the event statistics for neutron–proton interactions will be decisively enhanced allowing for a measurement of cascade baryon production.

16

References

[1] M. Botje et al. (NA49 Collab.), *Status and Future Programme of the NA49 Experiment* , CERN/SPSC 2000–011.

[2] M. Botje et al. (NA49 Collab.), *Additional Information Concerning Future NA49 Programme on Hadronic Physics with Proton and Pion Beams* , CERN/SPSC 2000–033.

[3] S. V. Afanasiev et al. (NA49 Collab.), *Study of the Onset of Deconfinement in Nucleus–Nucleus Collisions at Low SPS Energies*, CERN/SPSC 2000–035.

[4] S. V. Afanasiev et al. (NA49 Collab.), *Additional Information Concerning the Future of NA49 Programme on Nucleus–Nucleus Collisions at Low SPS Energies*, CERN/SPSC 2000–039.

[5] S. V. Afanasiev et al. (NA49 Collab.), *Status and Future of the NA49 Programme on Nucleus-Nucleus Collisions at SPS Energies*, CERN/SPSC 2001-008.

[6] S.Afanasev et al., Nucl. Inst. Meth. **A430** (1999) 210.

[7] M.Bleicher et al., hep-ph/0111187.

[8] F.Antinori et al., WA97 Collaboration, Nucl. Phys. **A661** (1999) 130c.

[9] T.Susa et al., NA49 Collaboration, Nucl. Phys. **A698** (2002) 491c.

[10] see: http://cern.web.cern.ch/CERN/Announcements/2000/NewStateMatter/

[11] for review see Proceedings of the 14th and 15th International Conference on Ultra–Relativistic Nucleus–Nucleus Collisions, Quark Matter 99, Nucl. Phys. **A661** (1999) 1c; Quark Matter 01, Nucl. Phys. **A698** (2002) 1c.

[12] review of QGP signatures: J.Harris and B.Müller, Annu. Rev. Nucl. Part. Sci. **46** (1996) 71.

[13] C.Hung and E.Shuryak, Phys. Rev. Lett. **75** (1995) 4003.

[14] M.Stephanov, K.Rajagopal and E.Shuryak, Phys. Rev. **D60** (1999) 114028.

[15] K.Rajagopal and F.Wilczek, Nucl. Phys. **399** (1993) 395; **B404** (1993) 557.

[16] D.Kharzeev, R.Pisarski and M.Tytgat, Phys. Rev. Lett. **81** (1998) 512.

[17] M. Gaździcki and M. I. Gorenstein, Acta Phys. Polon. **B30** (1999) 2705, and references therein.

[18] W. Cassing, E.L. Bratkovskaya and S. Juchem, Nucl. Phys. **A674** (2000) 249.

[19] F. Wang, H. Liu, H. Sorge, N. Xu and J. Yang, Phys. Rev. **C61** (2000) 064904.

[20] S. A. Bass et al., Prog. Part. Nucl. Phys. **41** (1998) 225; H. Weber et al. (UrQMD Collab.), to be published.

[21] J. Cleymans and K. Redlich, Phys. Rev. **C60** (1999) 054908,
P. Braun-Munzinger et al., Nucl. Phys. **A697** (2002) 902.

[22] U.Wiedemann and U.Heinz, Phys. Rept. **319** (1999) 145.

[23] Y.Sinyukov et al., Phys. Lett. **B432** (1998) 248.

[24] S.Jeon and V.Koch, Phys. Rev. Lett. **85** (2000) 2076.

[25] M.Asakawa, U.Heinz and B.Müller, Phys. Rev. Lett. **85** (2000) 2072.

[26] V.Koch, M.Bleicher and S.Jeon, Phys. Rev. **C62** (2000) 061902.

[27] E. V. Shuryak and M. A. Stephanov, Phys. Rev. **C63** (2001) 064903.

[28] J.Zaranek, preprint hep-ph/0111228 (Nov. 2001)

[29] M.Gaździcki, Eur. Phys. J. **C8** (1999) 131.

[30] A.Poskanzer and S.Voloshin, Phys. Rev. **C58** (1998) 1671.

[31] M. Gaździcki and Ch. Markert, Acta Phys.Polon. **B31** (2000) 965.

[32] M. Gorenstein et al., Phys. Lett. **B449** (1999) 401.

[33] P. Levai et al., J. Phys. **G27** (2001) 703.

[34] S. V. Afanasev et al. (NA49 Collab.), Phys. Lett. **B491** (2000) 59.

[35] M. C. Abreu et al. (NA50 Collab.), J. Phys., **G7** (2001) 405.

[36] E. Andersen et al., Phys. Lett. **B449** (1999) 401.

[37] S. V. Afanasiev et al. (NA49 Collab.), *Data Taking in 2002*, CERN/SPSC 2002-005/M677.
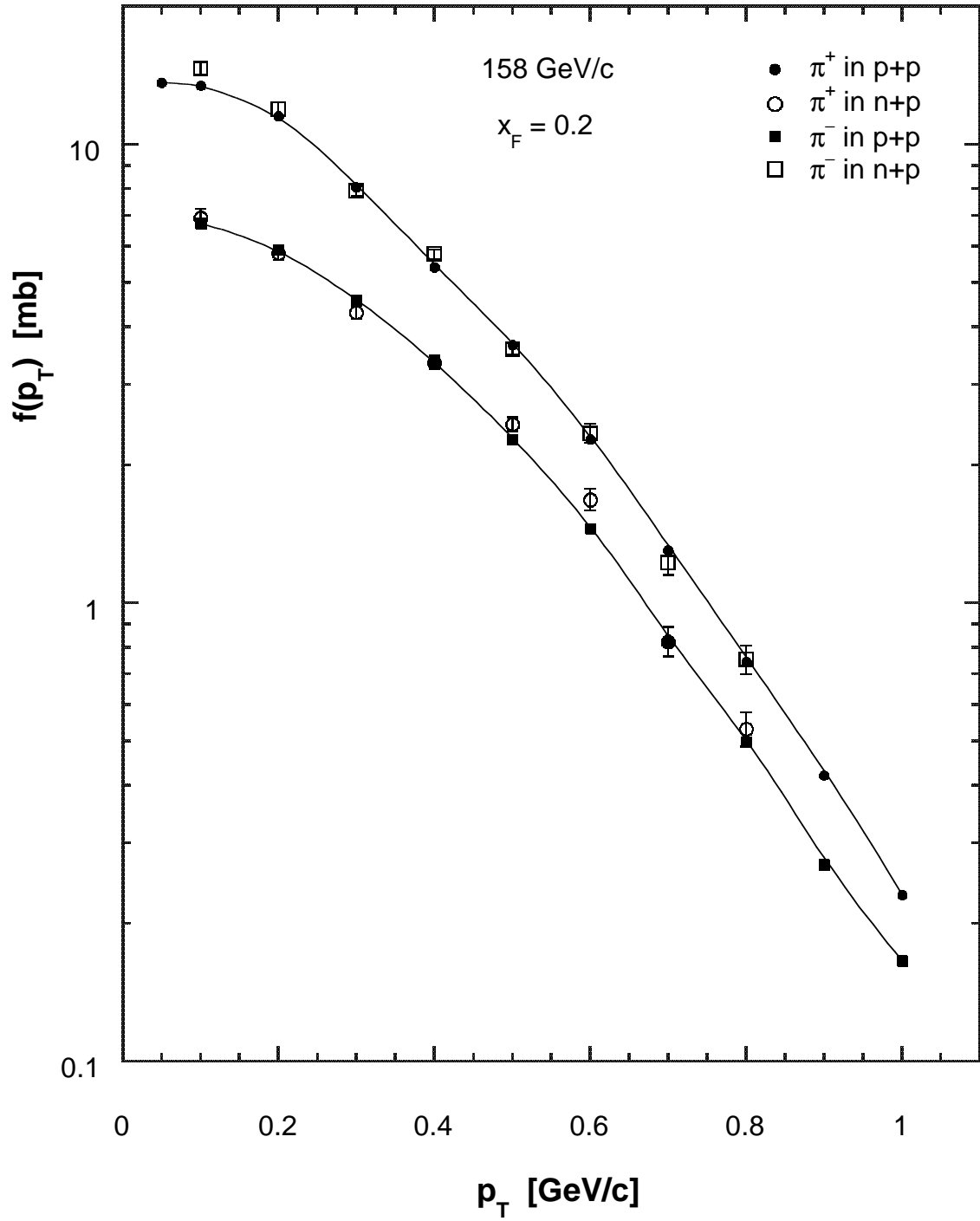
Figure 1: Differential invariant cross section as function of p_T at $x_F = 0.2$ for π^+ and π^- produced in p+p and n+p interactions.
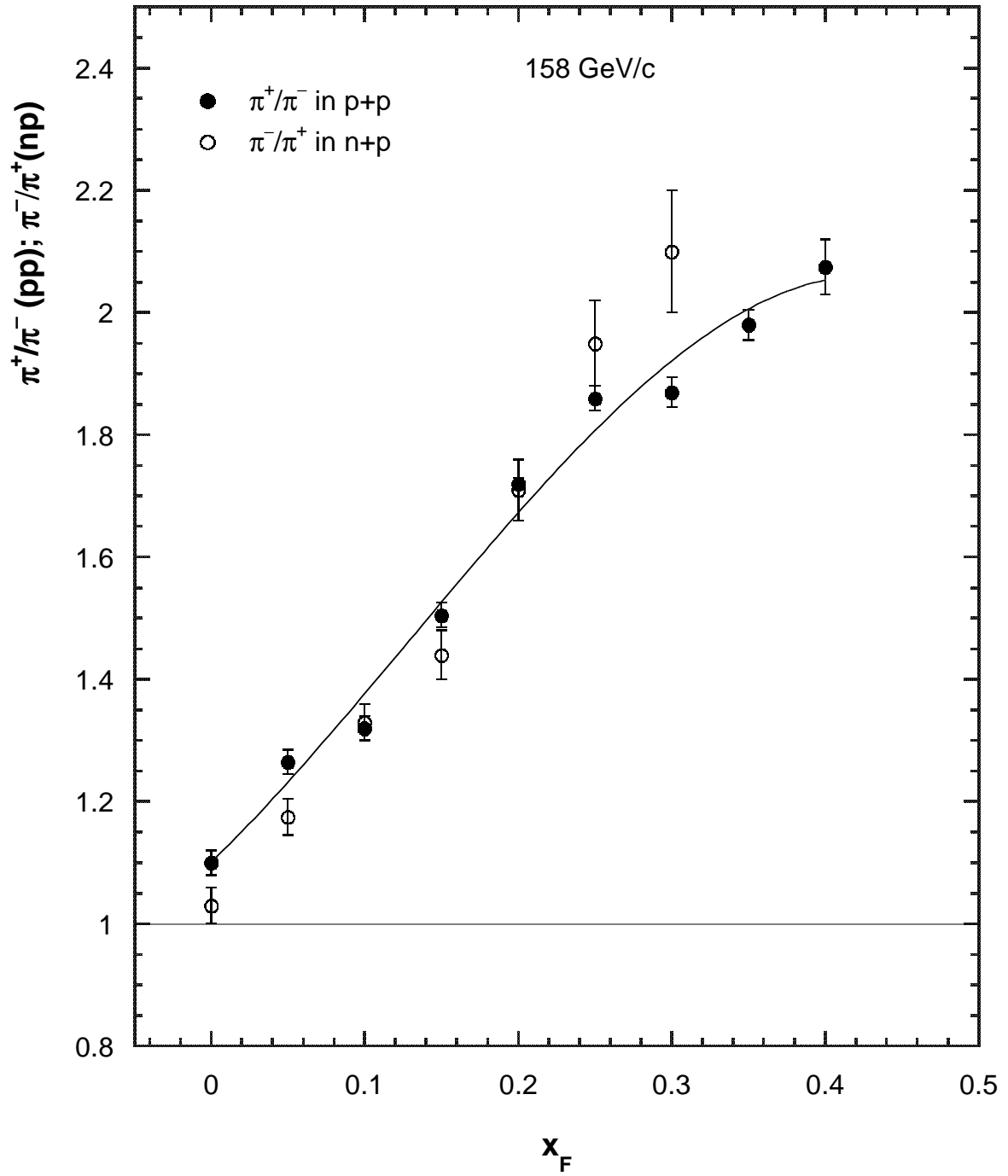
Figure 2: π^+/π^- ratio in p+p and π^-/π^+ ratio in n+p interactions as function of x_F.

20
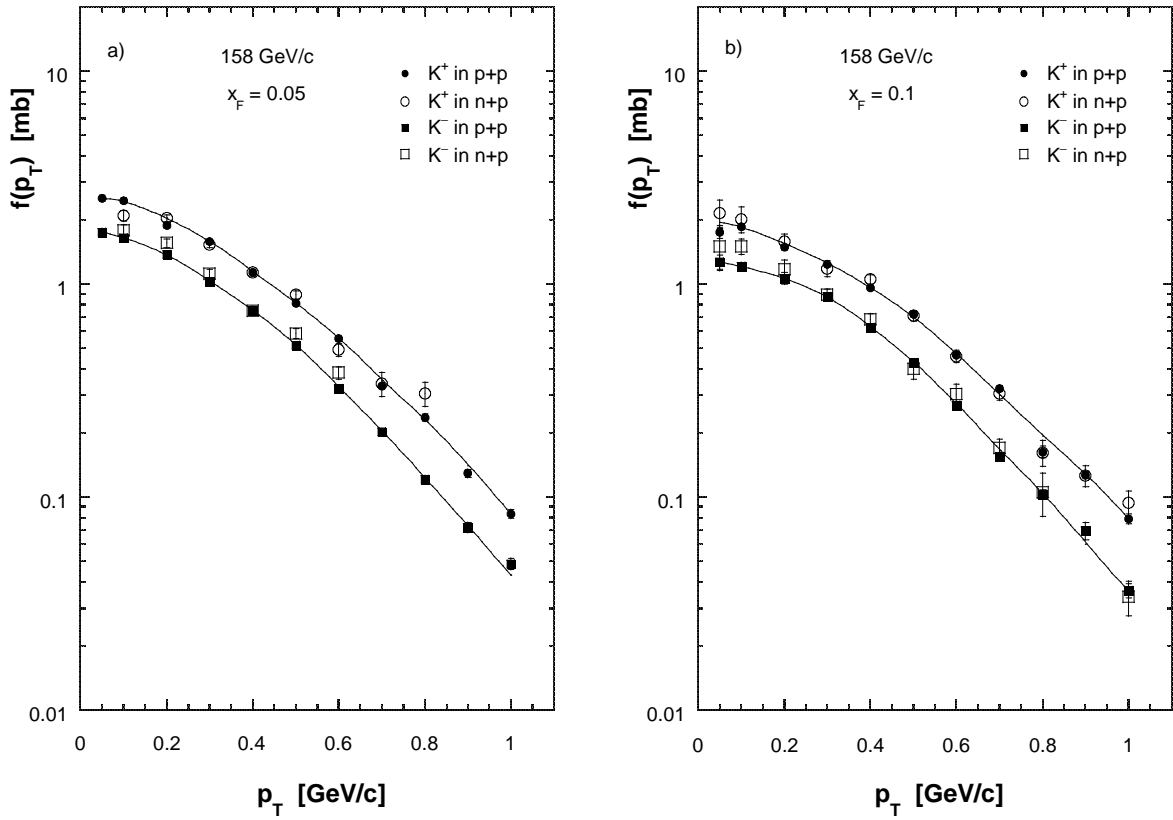
Figure 3: Differential invariant cross section as function of p_T at a) $x_F = 0.05$ b) $x_F = 0.1$ for K$^+$ and K$^-$ produced in p+p and n+p interactions.
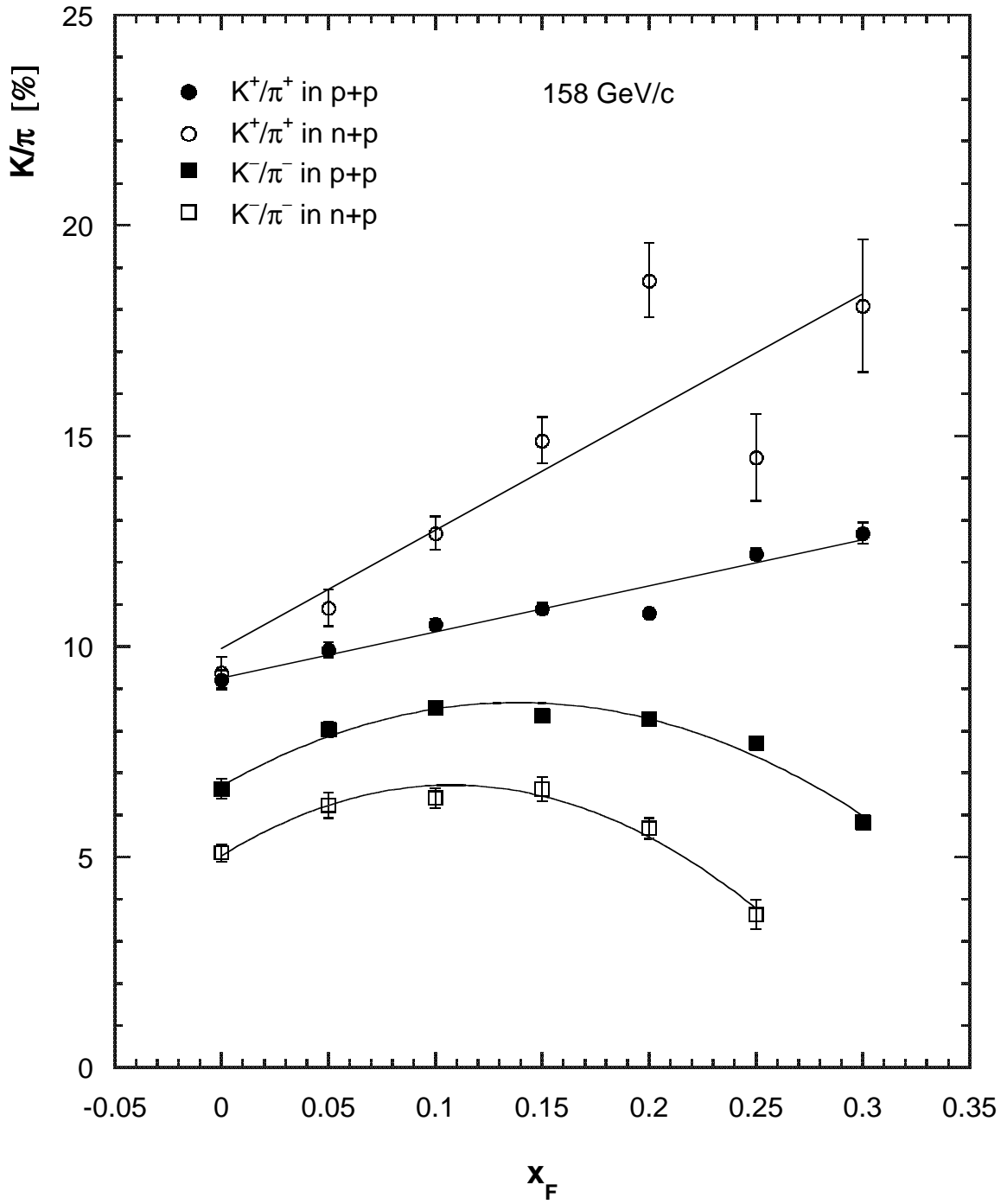
Figure 4: K^+/π^+ and K^-/π^- ratio as function of x_F in p+p and n+p interactions.
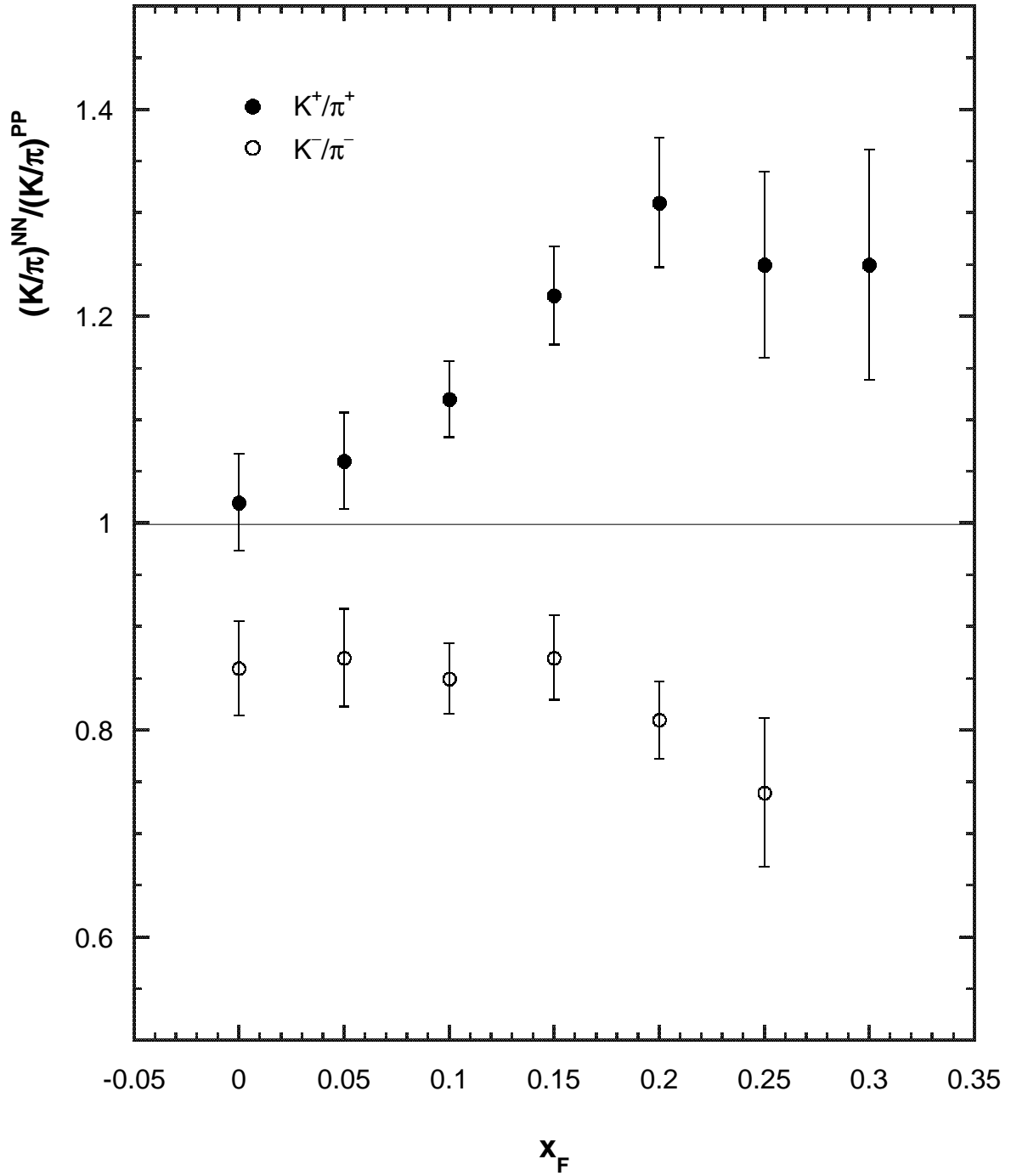
Figure 5: Ratios $(K^+/\pi^+)^{NN}/(K^+/\pi^+)^{pp}$ and $(K^-/\pi^-)^{NN}/(K^-/\pi^-)^{pp}$ as fuction of x_F representing the correction factors to be applied when comparing Pb+Pb and p+p interactions in order to account for the proper isospin composition of the Pb nucleus (60% n projectiles and 40% p projectiles).
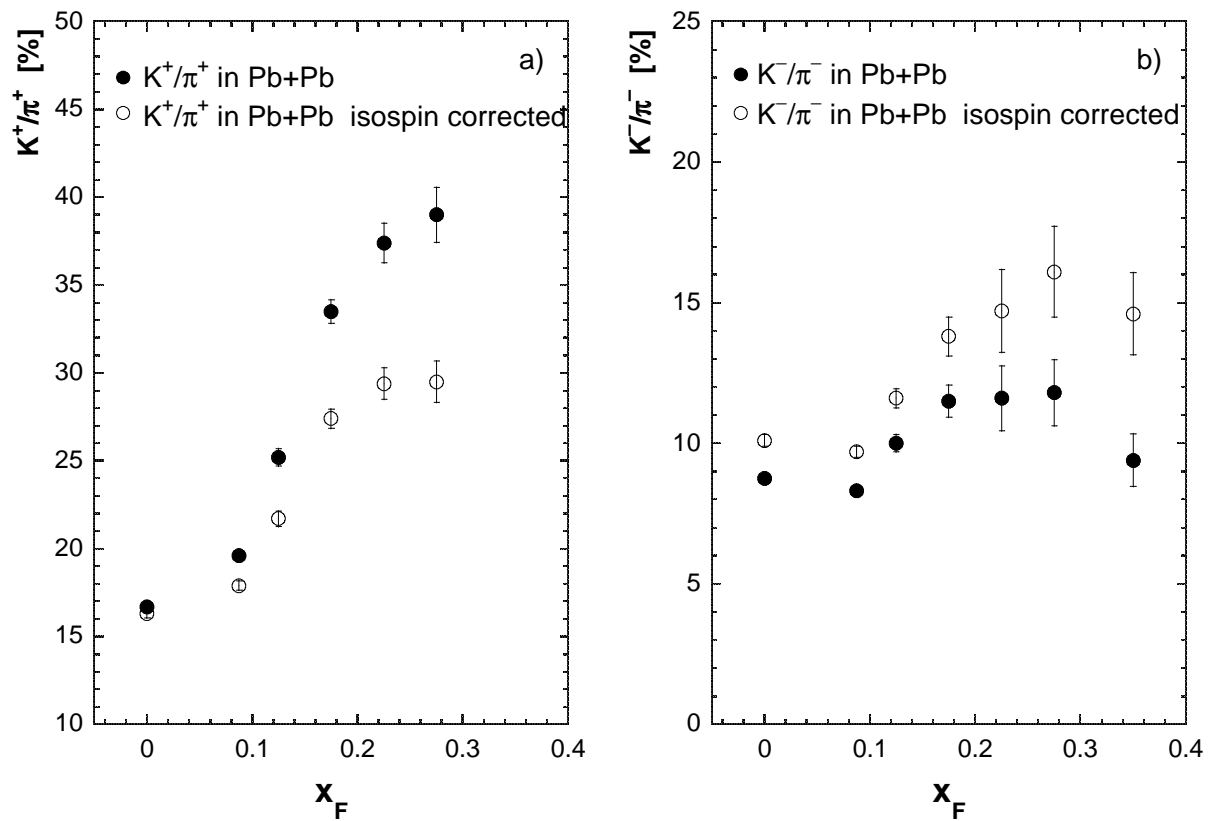
Figure 6: a) K^+/π^+ ratio b) K^-/π^- ratio as function of x_F for Pb+Pb collisions as measured and taking into account the proper isospin composition of the Pb nucleus (60% n projectiles and 40% p projectiles).
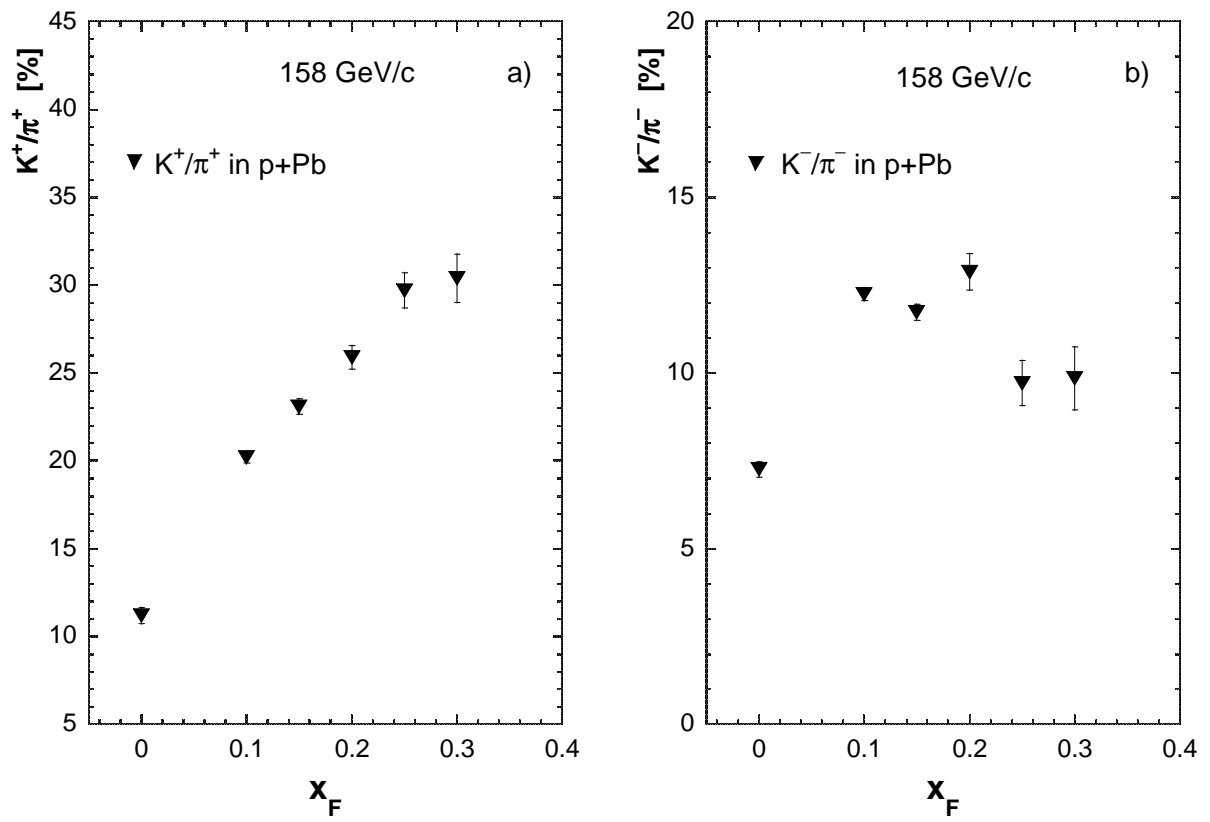
Figure 7: a) K^+/π^+ ratio b) K^-/π^- as function of x_F for p+Pb collisions.
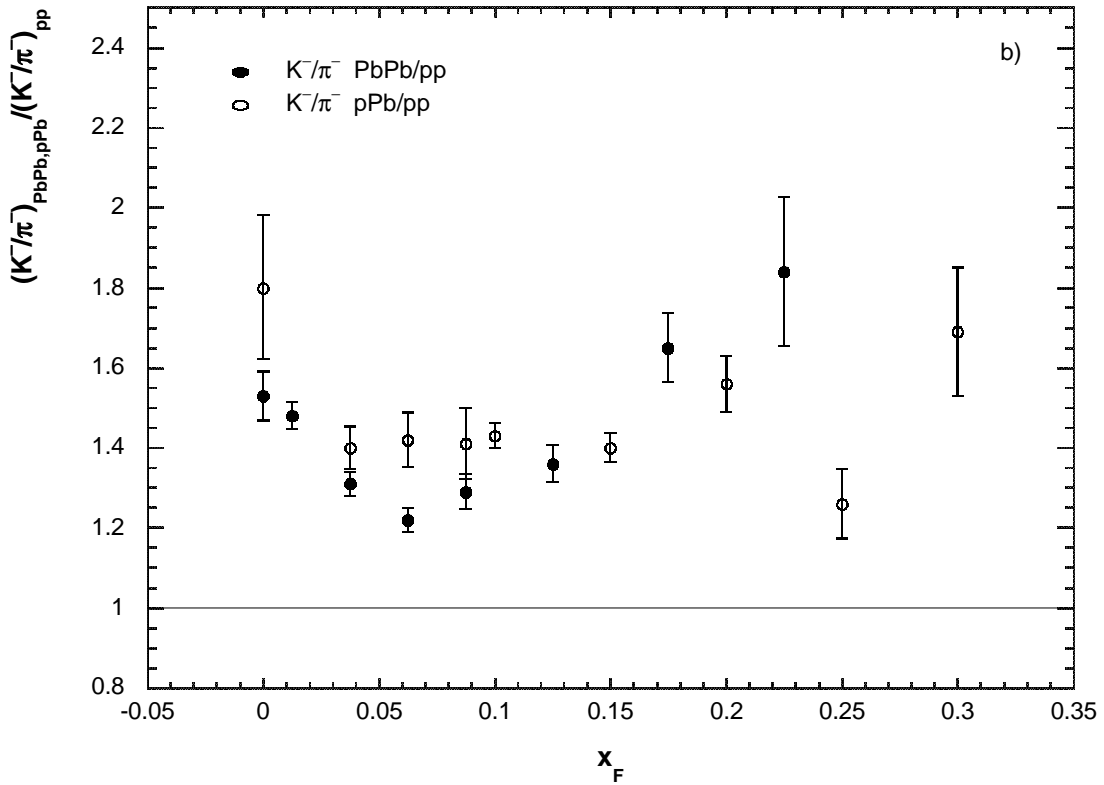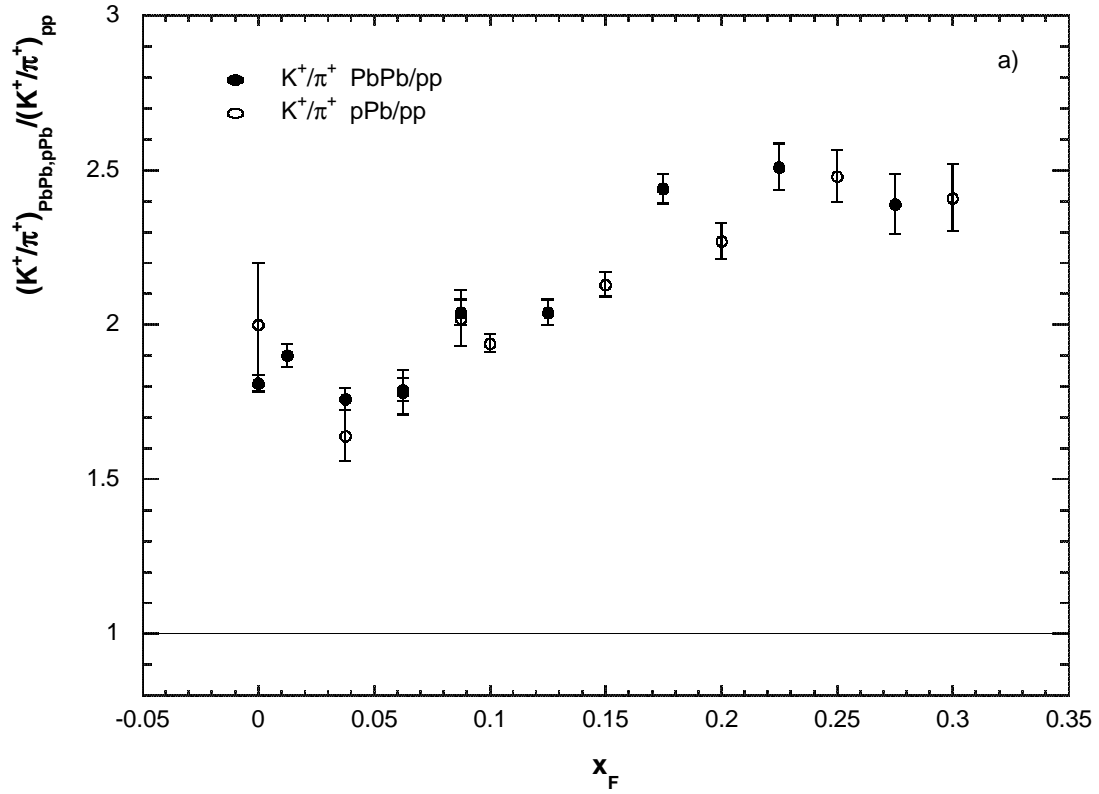
Figure 8: a) K^+/π^+ ratio b) K^-/π^- ratio as function of x_F for p+Pb and isospin corrected Pb+Pb collisions normalized to p+p interactions.

26
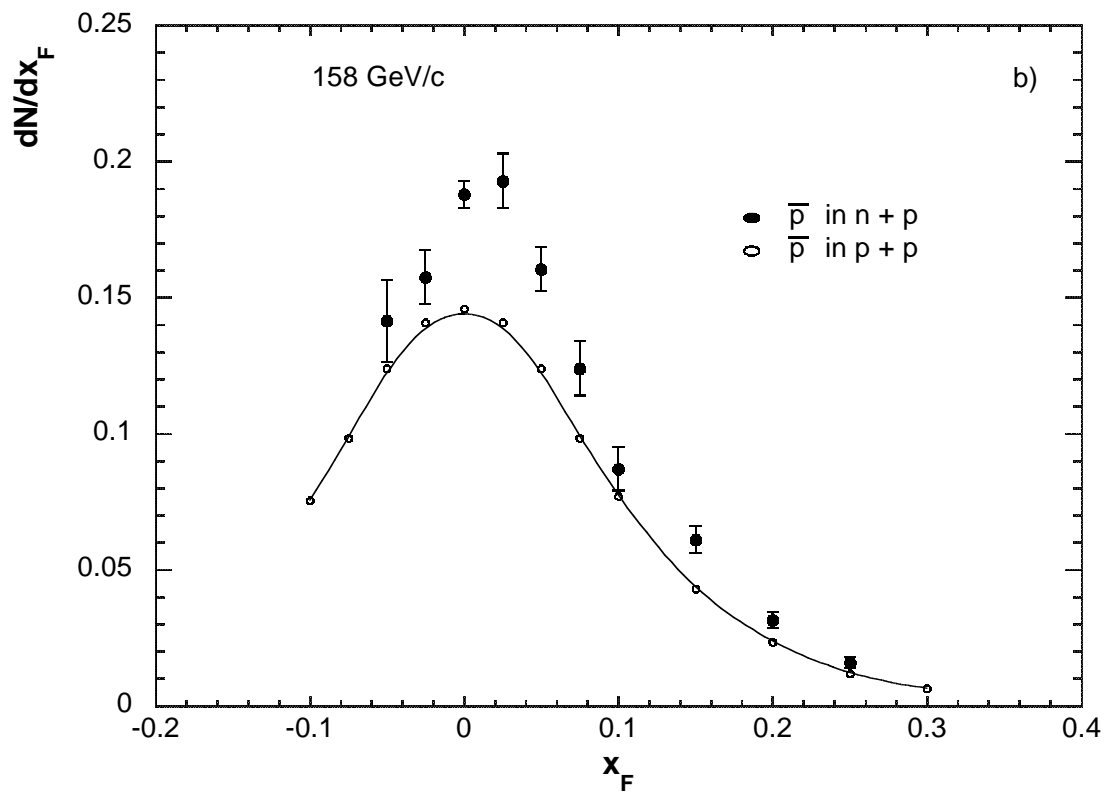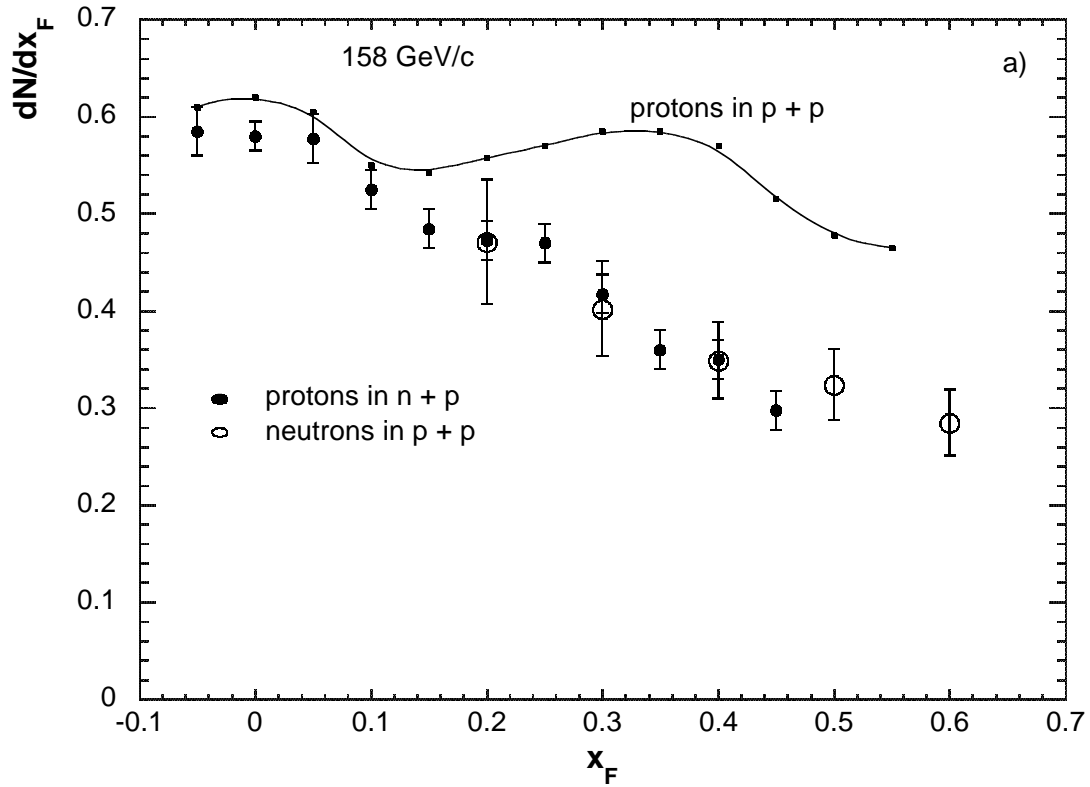
Figure 9: a) p yield as function of x_F for p+p and n+p interactions as well as n yield as function of x_F for p+p collisions; b) $\overline{p}$ yield as function of x_F for p+p and n+p interactions.
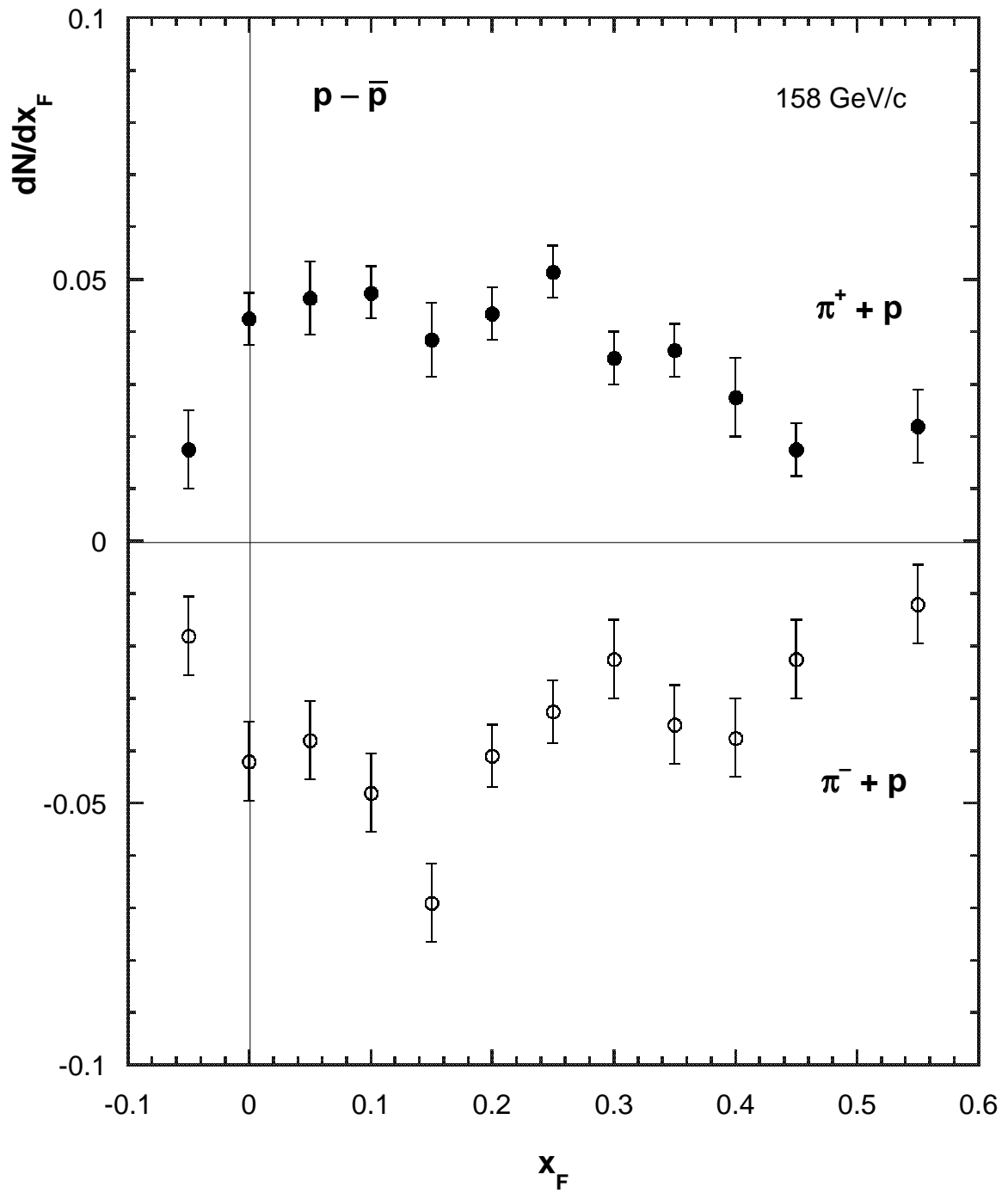
Figure 10: Target subtracted p–$\overline{\text{p}}$ yield as function of x_F for π^++p and π^-+p collisions.
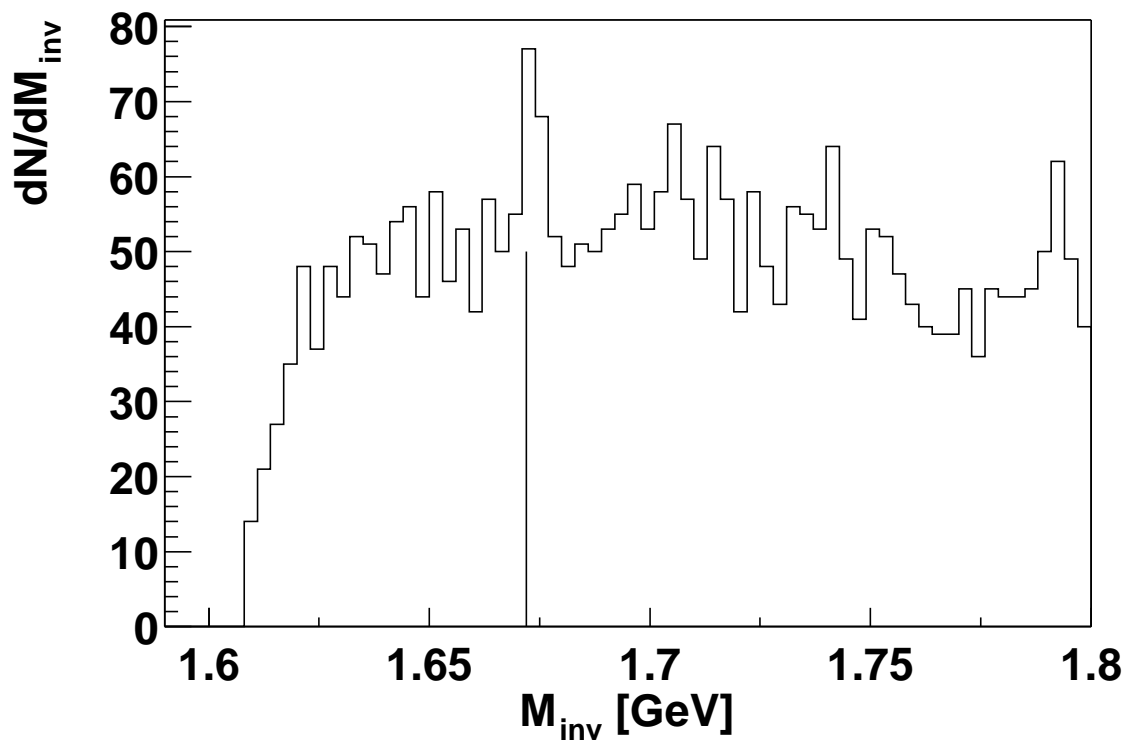
Figure 11: Observed Ω^- signal over background in p+p interactions at 158 GeV/c.
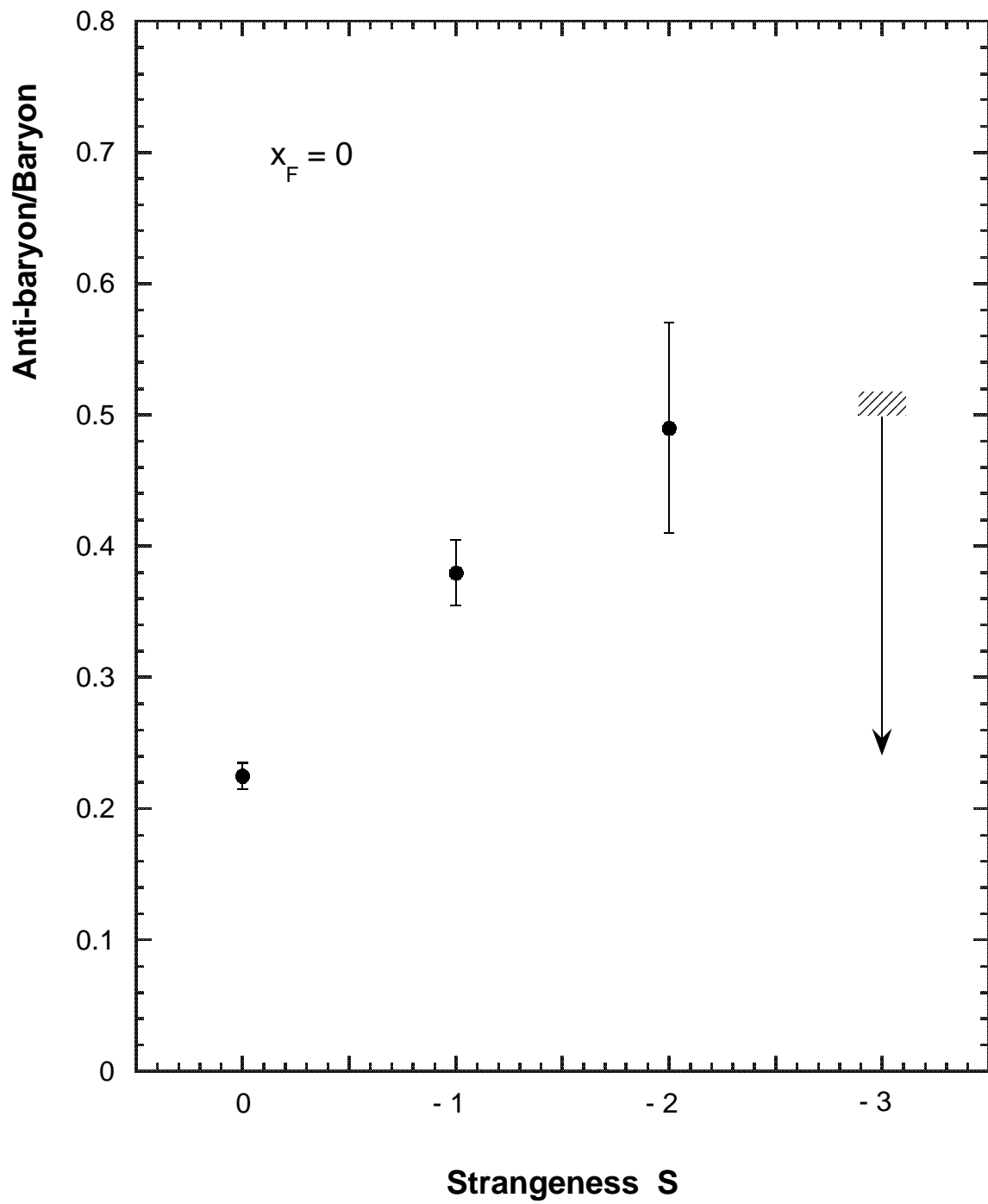
Figure 12: Baryon to Anti-baryon ratio at $x_F = 0$ as function of strangeness content.
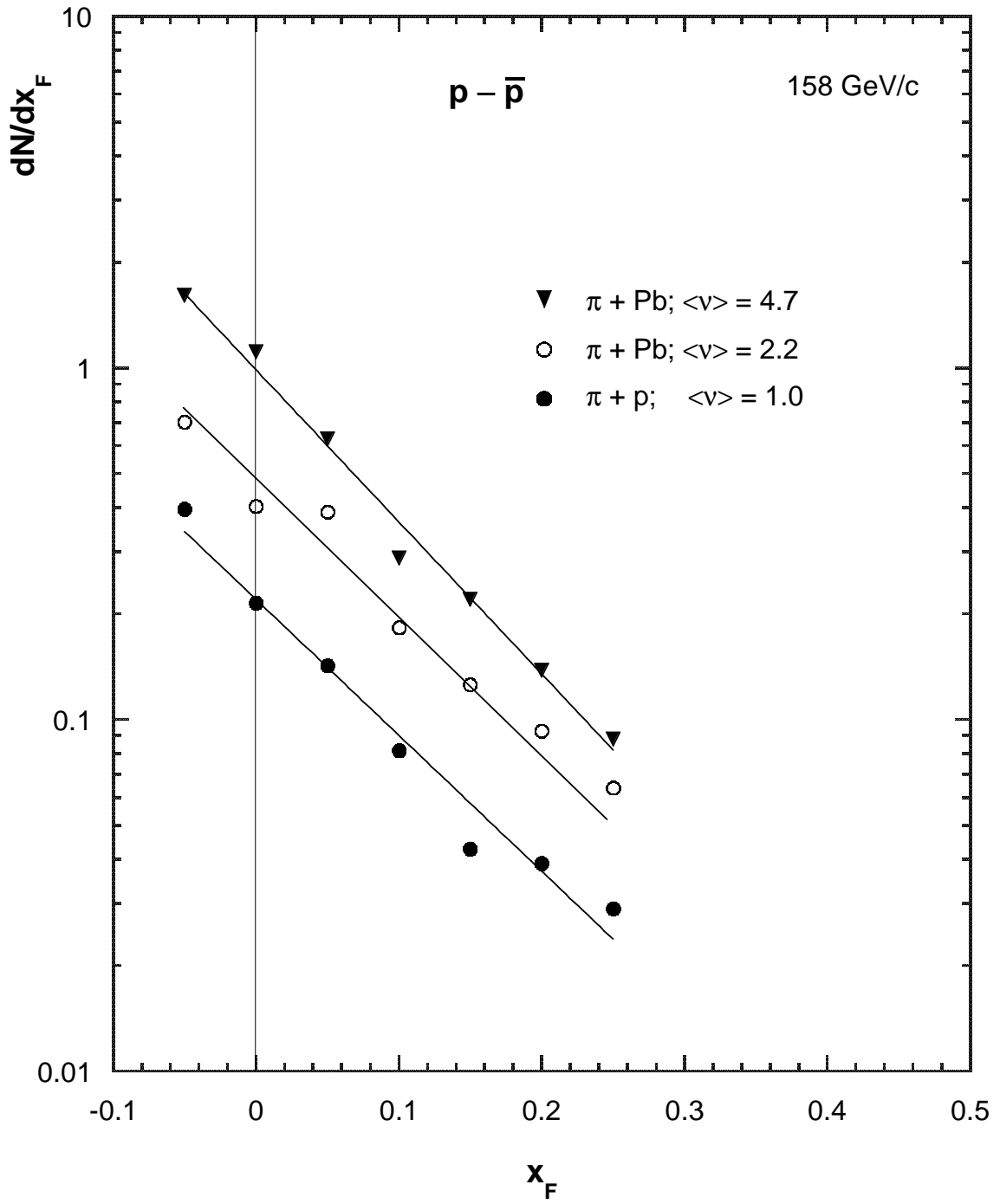
Figure 13: p–$\overline{\text{p}}$ yield as function of x_F for π+Pb interactions at different centralities, i.e. different mean number of collisions $\langle \nu \rangle$, and π+p collisions ($\langle \nu \rangle = 1$).
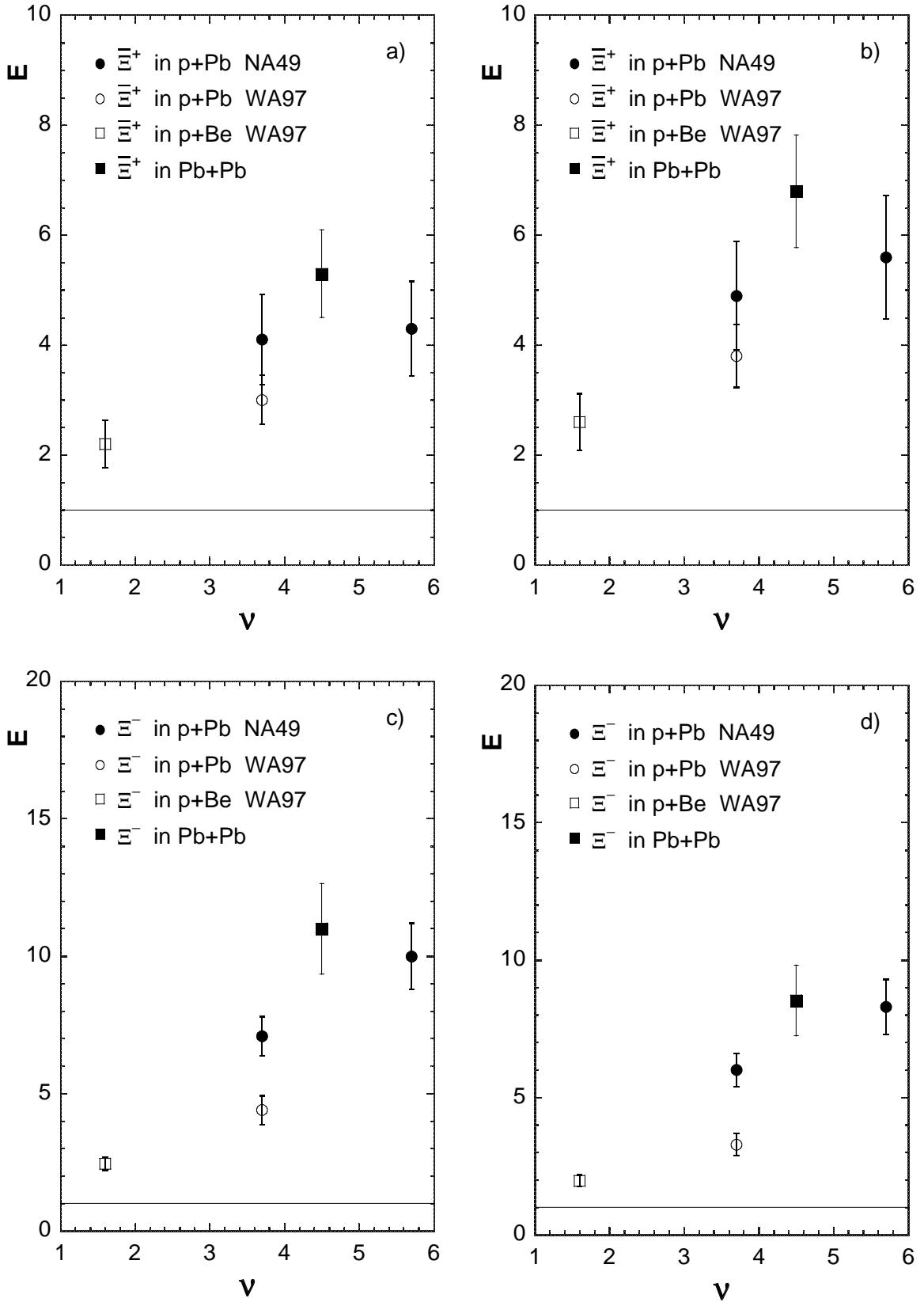
Figure 14: Enhancement factor for the production of a) Ξ^+ and c) Ξ^- as measured and b), d) taking into account the isospin correction deduced from p and $\bar{p}$ yields of p+p and n+p collisions.
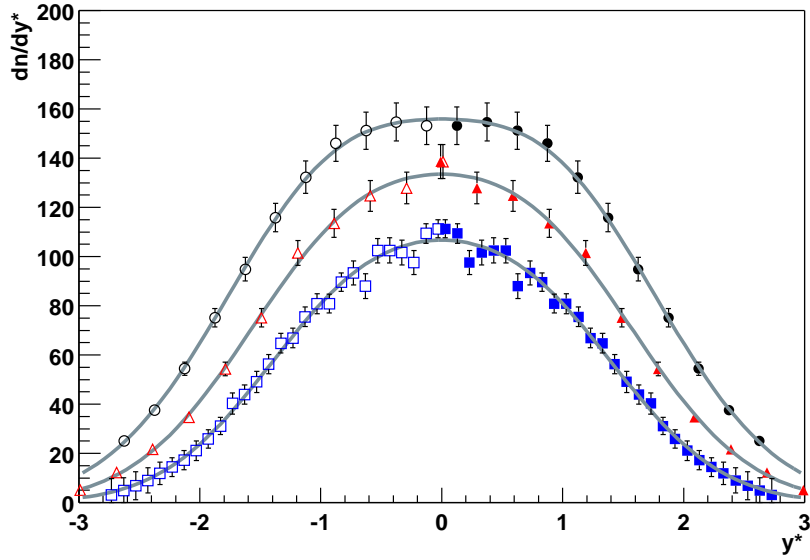
Figure 15: Rapidity distribution of π^- in central Pb+Pb collisions at 40 (squares), 80 (triangles) and 158 (dots) A·GeV. Open symbols show values reflected at $y^\star=0$ (NA49 preliminary).
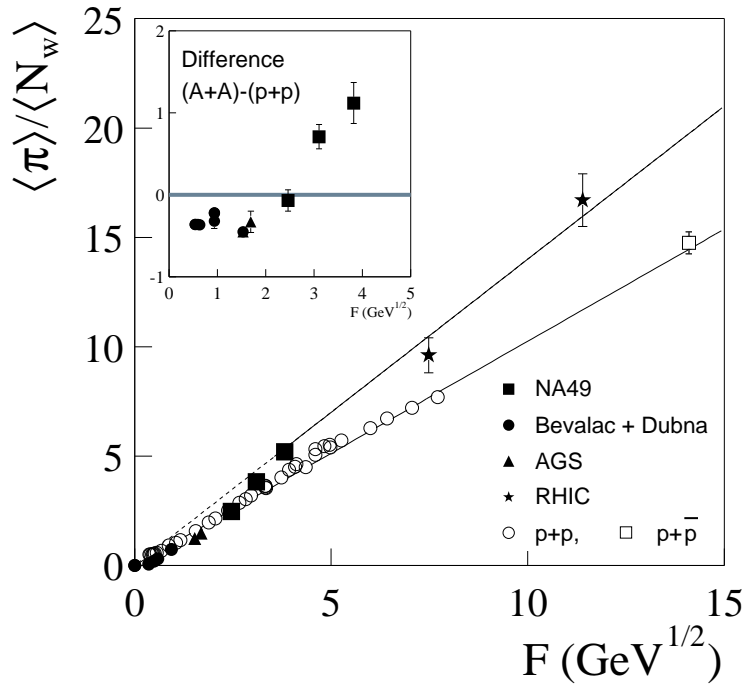
Figure 16: Total pion multiplicity $\langle\pi\rangle$ produced per wounded (participant) nucleon versus the Fermi energy variable $F \approx s_{NN}^{0.25}$ for p+p reactions (open symbols) and central nucleus–nucleus collisions (full symbols).
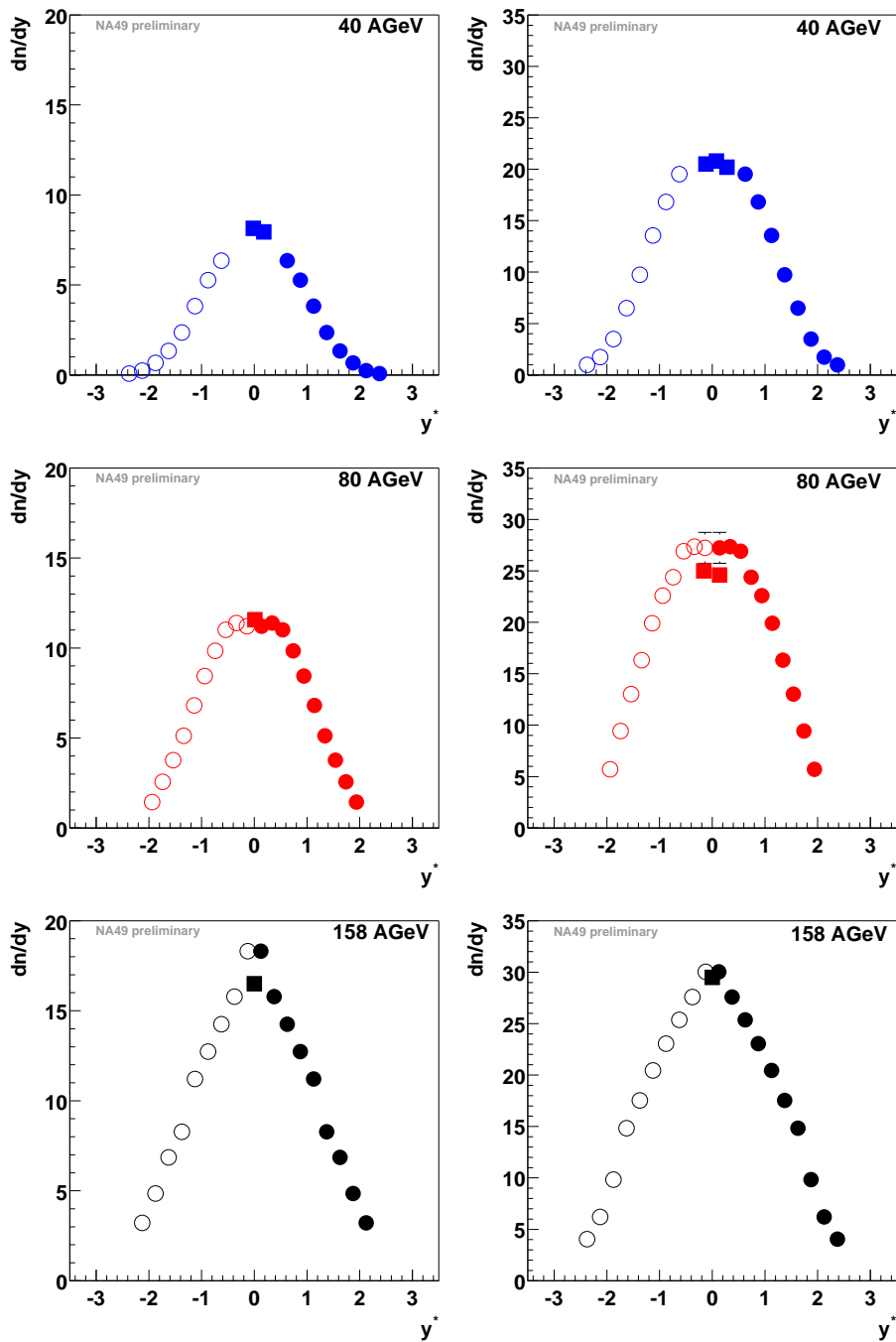
Figure 17: Rapidity distribution of K$^-$ (left) and K$^+$ (right) from dE/dx (circles) and combined dE/dx and TOF (squares) analysis. Open symbols show values reflected at y*=0. (NA49 preliminary)
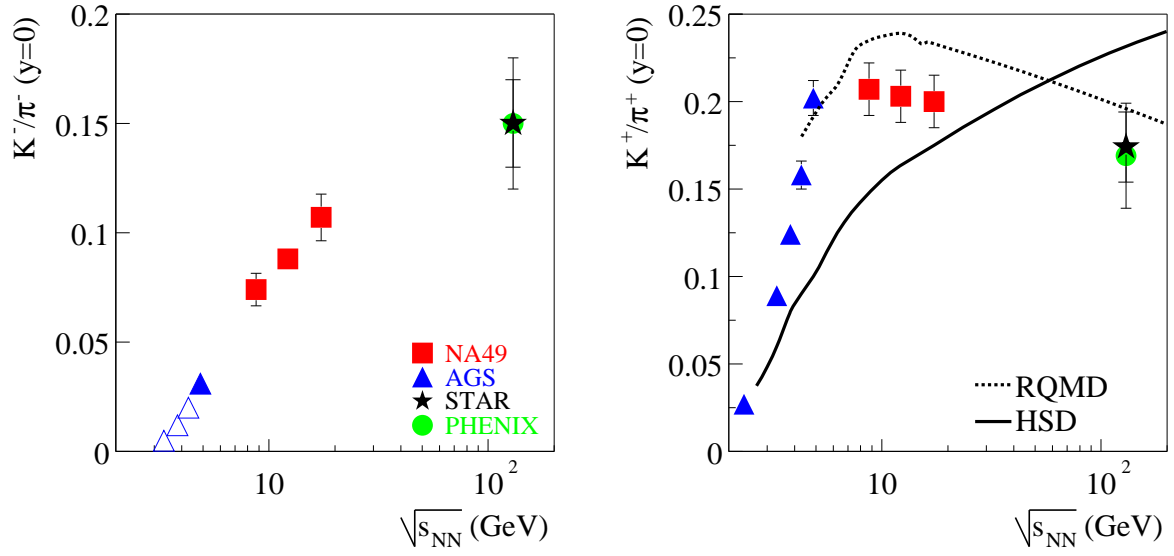
Figure 18: Midrapidity ratio of K^-/π^- (left) and K^+/π^+ (right) as function of energy from NA49 (squares, preliminary) compared to measurements at lower and higher energies. Predictions of the RQMD [19] (dotted) and HSD [18] (full curve) models are shown.
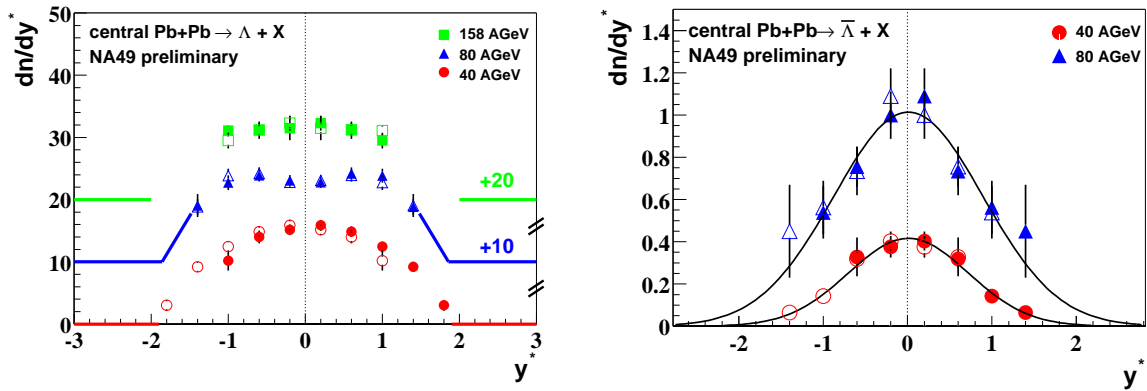
Figure 19: Rapidity distribution of Λ (left) and $\bar{\Lambda}$ (right). Open symbols show values reflected at $y^\star=0$. Λ yields at 80 and 158 A·GeV are displaced vertically by 10 respectively 20 units for clarity. (NA49 preliminary)
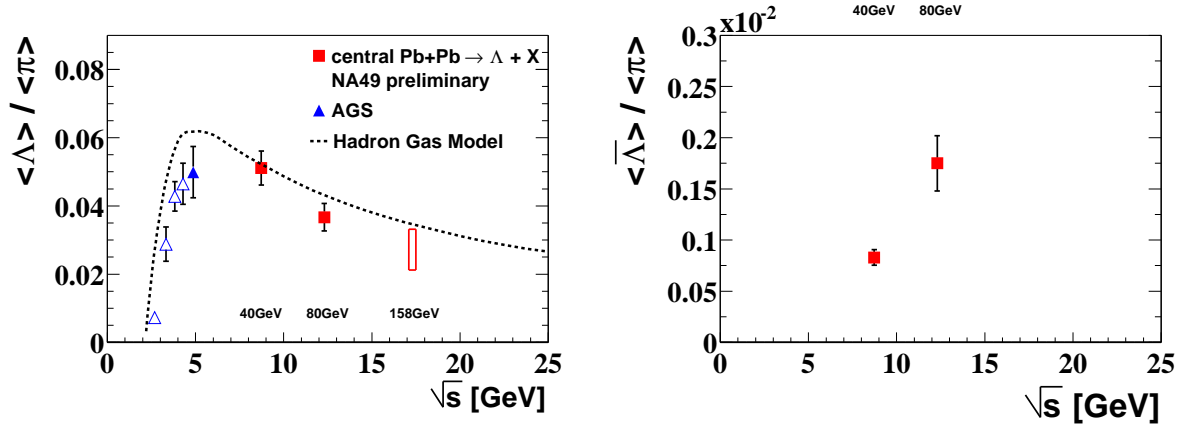
Figure 20: 4π yield ratios $\langle\Lambda\rangle/\langle\pi\rangle$ (left) and $\langle\bar{\Lambda}\rangle/\langle\pi\rangle$ (right) versus energy from NA49 (squares, preliminary) and lower energy AGS experiments. The dotted line shows a prediction from the extended hadron gas model [21].
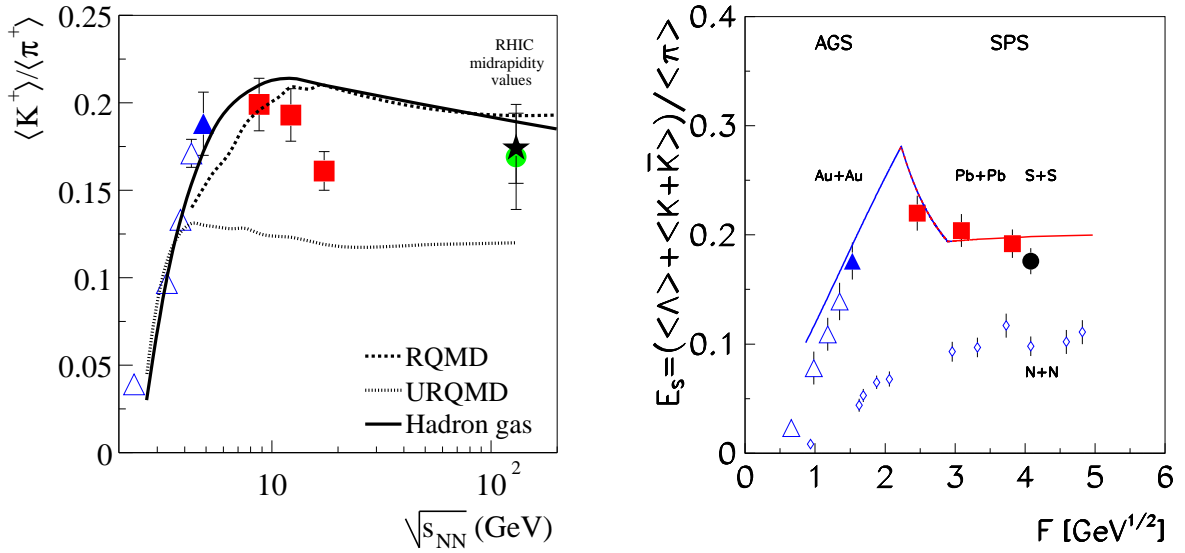
Figure 21: Left: 4π ratio $\langle K^+\rangle/\langle\pi^+\rangle$ versus energy compared to predictions of the RQMD [19] (dashed), UrQMD [20] (dotted) and extended statistical [21] (solid curve) models. Right: the strangeness content measure E_s versus the Fermi energy variable $F\approx s_{NN}^{0.25}$ compared to the prediction of the statistical model of the early stage [17] (curves).
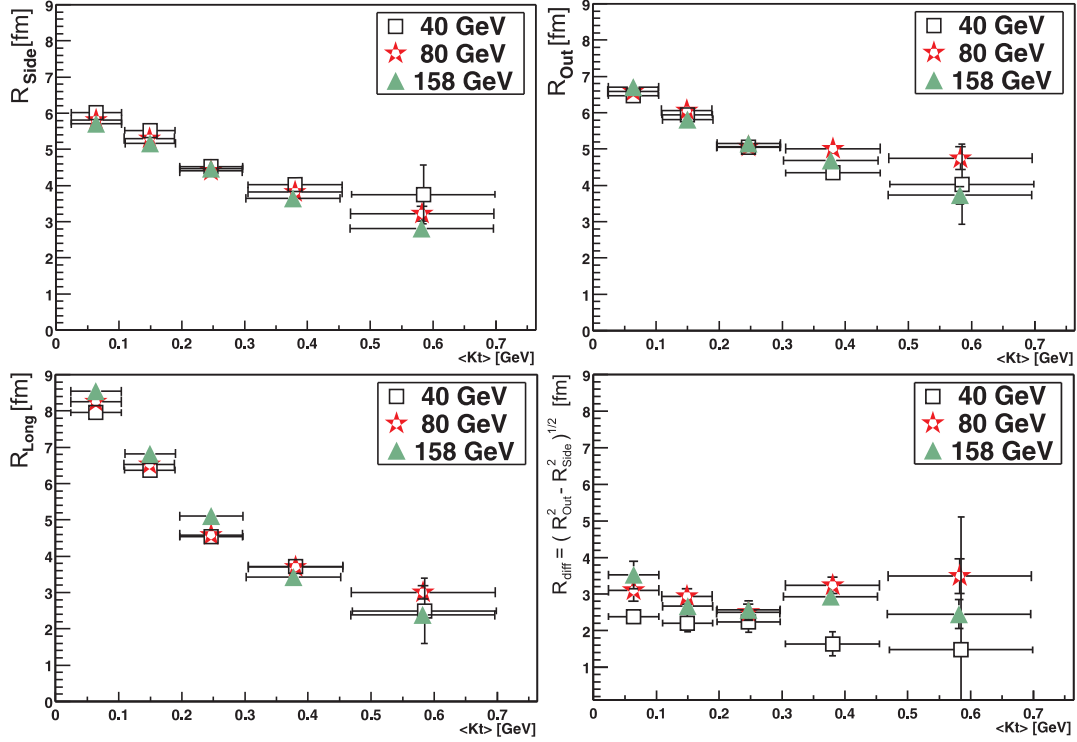
Figure 22: Gaussian radius parameters R_{side}, R_{out}, R_{long} fitted to the $\pi^-\pi^-$ correlation function evaluated in the longitudinally comoving frame plotted versus the average transverse momentum K_T of the pair. Rapidity range $y^\star \leq y \leq y^\star + 0.5$ (NA49 preliminary).
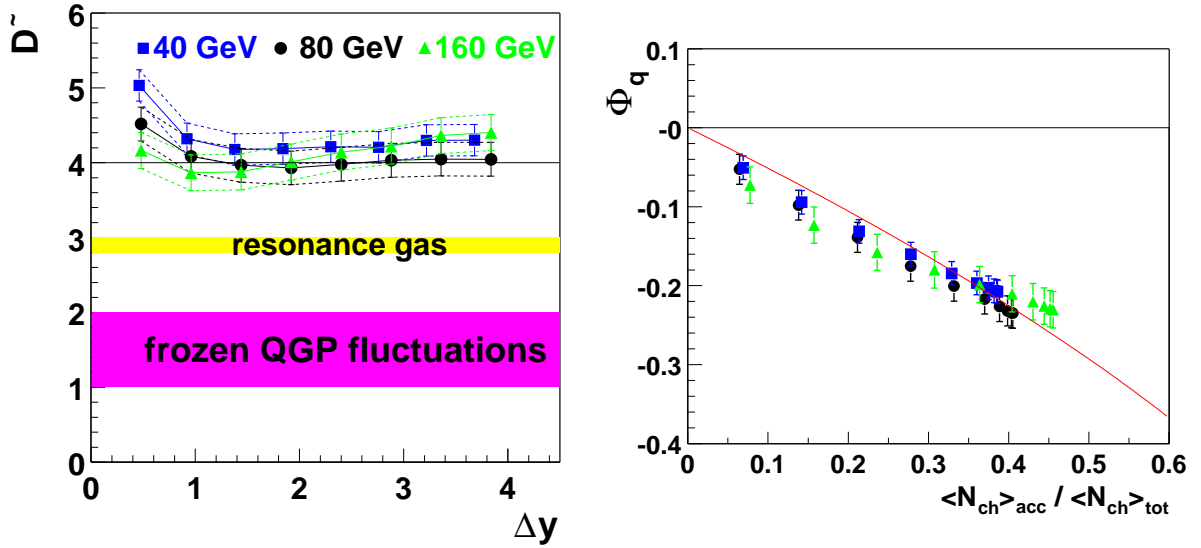

Figure 23: Measures of event-to-event charge fluctuations in central Pb+Pb collisions. Left: $\tilde{D}$ versus the size of the rapidity window Δy. Right: Φ_q versus the ratio $\langle N_{ch}\rangle/\langle N_{ch}\rangle_{tot}$ of the multiplicity in the acceptance window and the total multiplicity in the events; the curve shows the prediction for independent particle emission plus global charge conservation (NA49 preliminary).
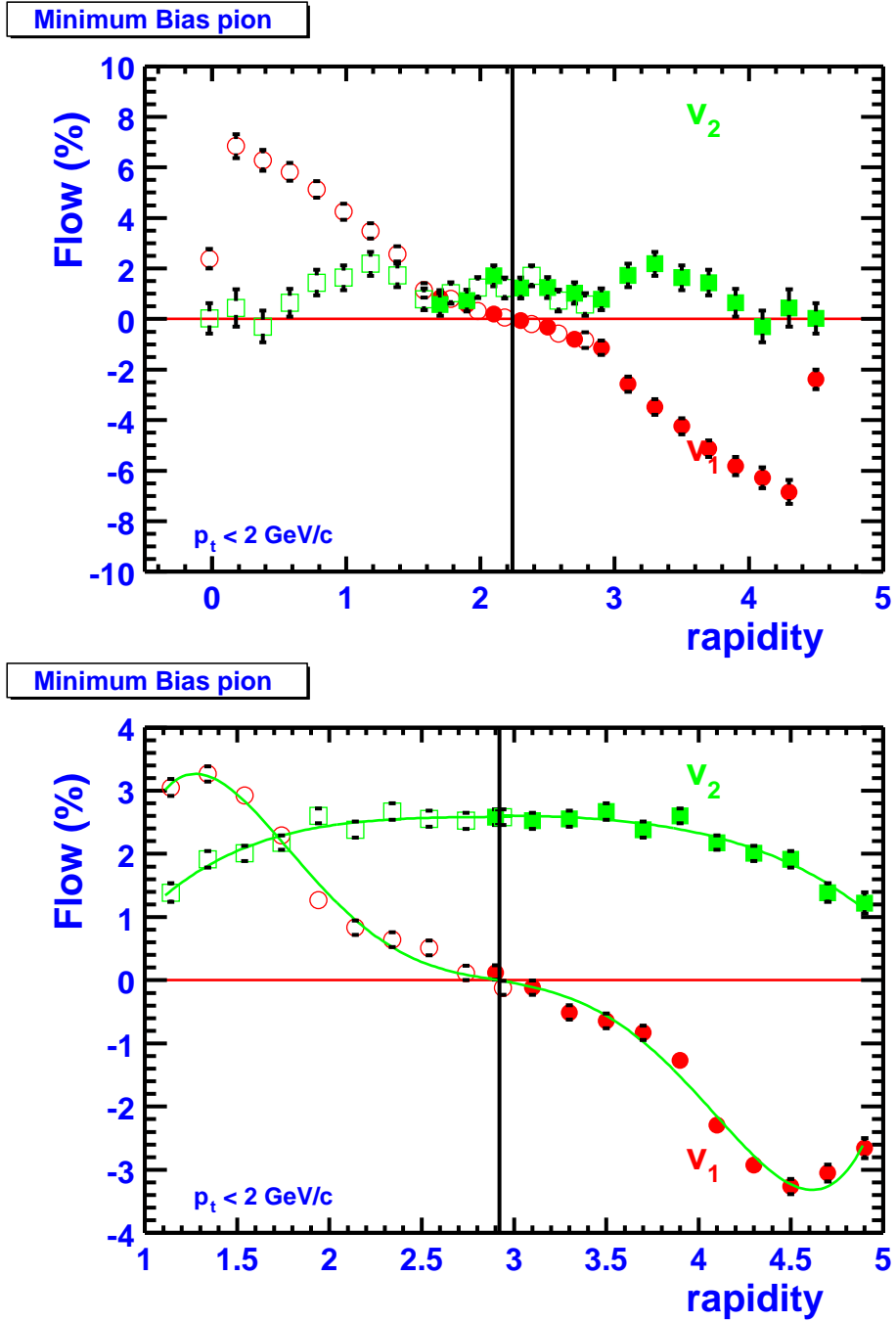
Figure 24: Fourier coefficients v_1 (directed flow) and v_2 (elliptic flow) of the azimuthal distribution of pions in min.bias Pb+Pb collisions versus the rapidity at 40 (left) and 158 (right) A·GeV beam energy (NA49 preliminary).
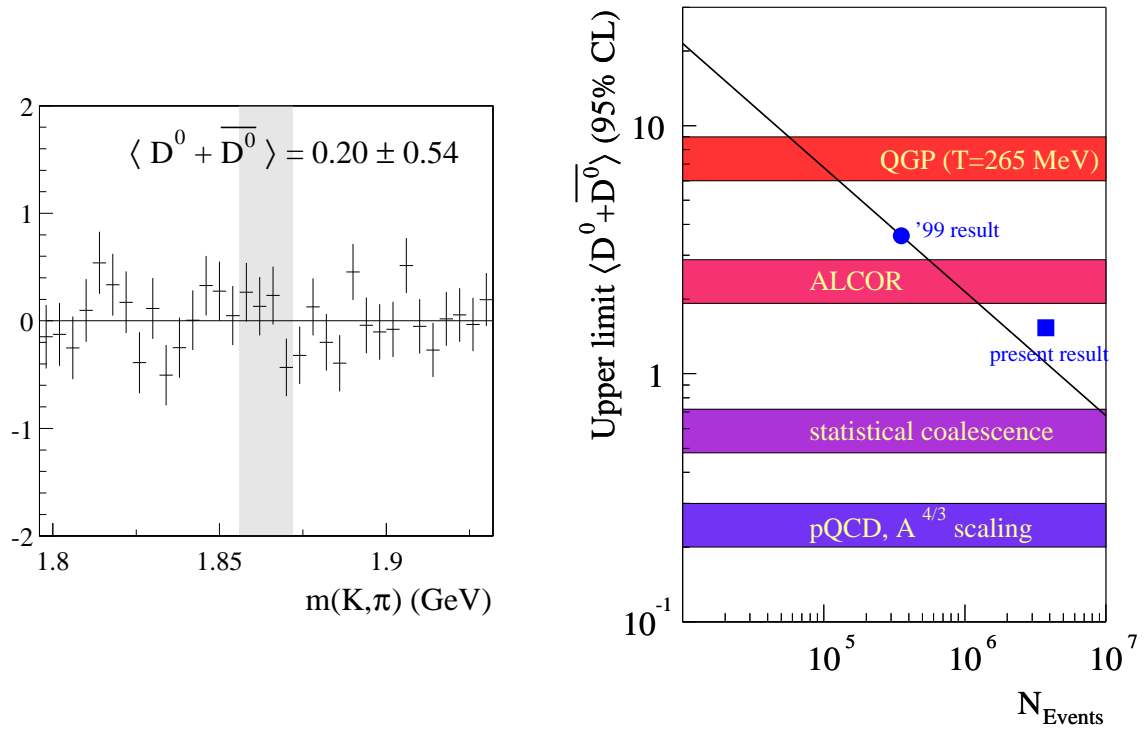
Figure 25: The invariant mass spectrum for $K - \pi$ pairs after background subtraction in the region of the expected signal from D^0 and $\overline{D}^0$ decays (left). The values are corrected for acceptance and branching ratio. The upper limit for the $D^0 + \overline{D}^0$ yield measured for central Pb+Pb collisions at 158 A·GeV (right). The predictions of various models are also given (NA49 preliminary).
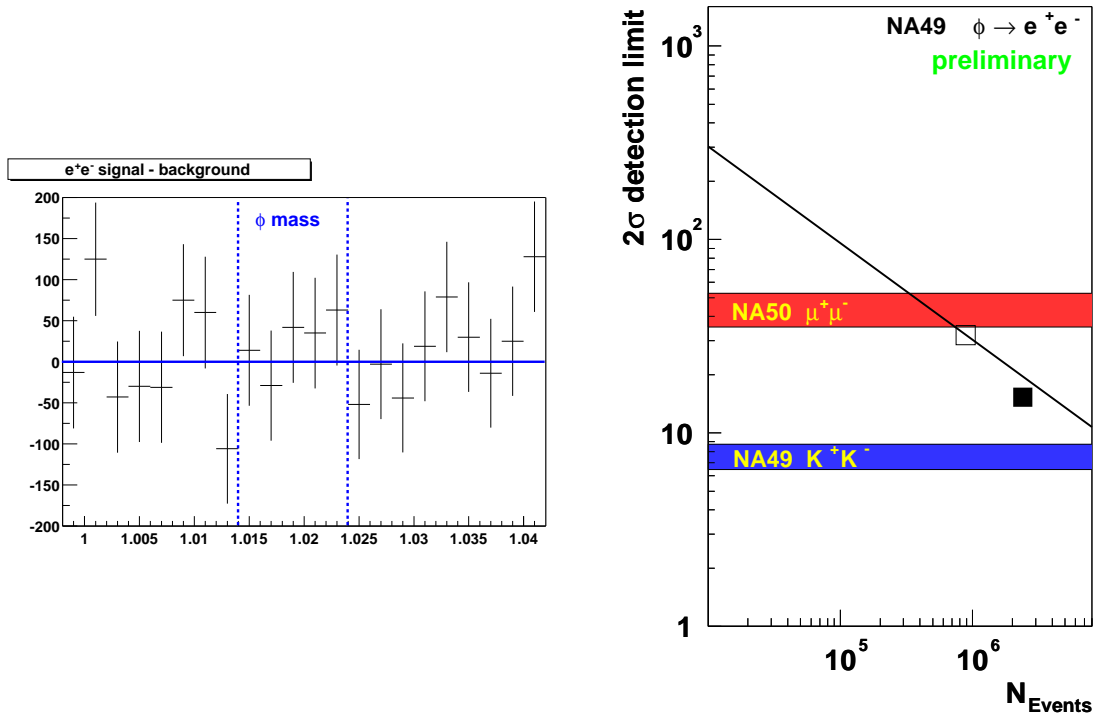
Figure 26: The invariant mass spectrum for $e^+ - e^-$ pairs after background subtraction in the region of the expected signal from ϕ decays (left). Upper limits for the total ϕ multiplicity per event measured via the dielectron channel for central Pb+Pb collisions at 158 A·GeV (right): result from 1996 data (800K events) is shown by open square, from 2000 data (2.4M events) by full square. The multiplicity derived from the dimuon and $K^+ + K^-$ channels are indicated by the upper and lower horizontal bands respectively (NA49 preliminary).
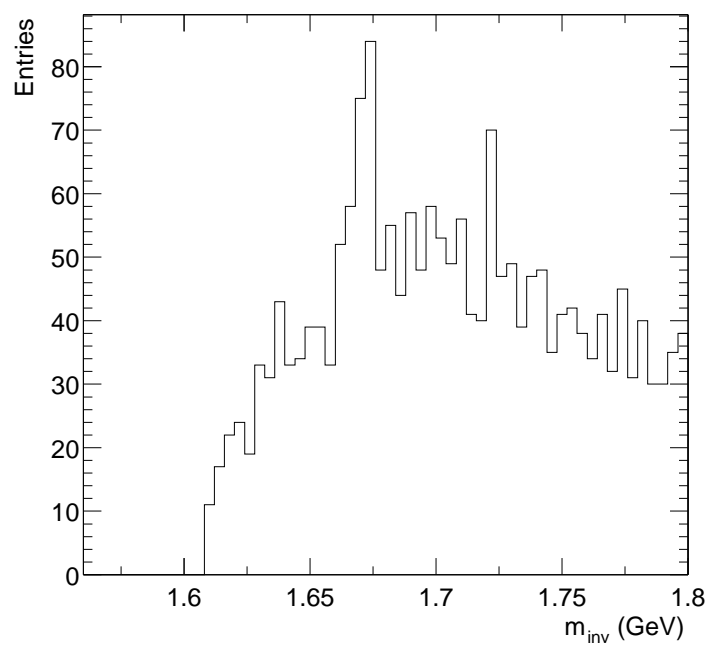
Figure 27: The preliminary invariant mass distribution of pairs of Λ and kaon candidates in the mass region of the Ω as measured in 500k central Pb+Pb events at 158 AGeV. A clear Ω signal is observed at the correct position (NA49 preliminary).